Spring 5-2015

A Paleolimnological Study Reconstructing Organic Carbon Accumulation and Climate History; Mealy Mountains, Labrador, Canada

Timothy D. Campbell
Bates College, tcampbel@bates.edu

A Paleolimnological Study Reconstructing Organic Carbon Accumulation and Climate History; Mealy Mountains, Labrador, Canada

Bates College Geology Department Thesis

Presented to the Faculty of the Department of Geology, Bates College,
in partial fulfillment of the requirements for the Degree of Bachelor of Science

by
Timothy D. Campbell

Lewiston, Maine
April 8th, 2015

Abstract

Over the past century, the global climate system has experienced unprecedented warming due to the rapid increase of greenhouse gas concentrations. Thus, understanding the fate of CO_2 once it is released is critical to evaluating the impacts of future climate change. Lake sediments have the potential to store large quantities of CO_2 in the form of organic carbon, yet the factors which control organic carbon burial efficiency in lakes are not fully understood. Consequently, this project examines the sedimentary record from one lake spanning the boreal forest-tundra ecotone in the eastern Mealy Mountains of southeastern Labrador, Canada in order to identify lake and watershed controls on organic carbon accumulation and evaluate the sensitivity of organic matter accumulation to changing climatic conditions. The pronounced environmental gradient and significant post-glacial environmental changes in this region provide an ideal setting for testing controls on organic matter accumulation.

This study presents results of a multi-proxy reconstruction of one sediment record recovered from a lake located in the Mealy Mountains (53°N, 58°W). Proxies used in this study included % organics (%LOI, %C, and %N), XRF elemental analysis, magnetic susceptibility, and fossil pigment paleoproductivity reconstruction. In order to evaluate changes in mass accumulation rate of organic carbon, two age models were generated based on seven radiocarbon dates.

Contained within the sediment core collected from Moose Lake (ML-14-2) are three distinct lithostratigraphic units: unit A, B, and C. The top unit is described as a homogenous, organic rich gyttja that transitions into an inorganic, clastic unit containing both silt and clay. This visual classification of the core stratigraphy is further reflected by the several geochemical analysis used in this study and suggests that Moose Lake experienced a major shift in sediment accumulation and paleoproductivty ca. 6000 cal ye BP. Fossil pigment concentrations, which reflect rates of productivity, where highest in the inorganic unit. This suggests that fossil pigments may not be a good predictor of organic material accumulation. MAR of organic materials suggest that although accumulation rates of carbon are low, they may be sensitive to change in climate.

Acknowledgments

Starting with the field work and culminating in this final piece of writing, this project as truly been one of the hardest and most demanding experiences of my life. Over the course of the past year, I have been challenged physically, mentally, and academically in ways I have never before. It is almost a surprise that I find myself near completing at this final hour. Throughout the duration of this project, several amazing individuals donated their time, energy, and support. If were not for these people, completing this project would have been near impossible. Here is to those individuals:

First, I would like to thank the Bates College Student Research Fund for providing me the opportunity to take part in this project as well as the Donors of the American Chemical Society Petroleum Research Fund for partial support of this research.

To my fellow field partner, Dan Cronin; I truly don't believe I would have been able to survive the three weeks in Labrador without you.

To Tim Cook, thank you for welcoming aboard this project and for guiding me in the right direction along the way.

To Mike Retelle, ever since I took Quaternary with you sophomore year, I have admired your passion and enthusiasm for your work in addition to your genuine love for the study of the earth system and to educate others about it. Thank you for everything.

To Phil, Bill, and Holly, thank you for going out of your way to help me with some of the puzzles that this project has consisted of.

To my fellow seniors and Bates geologists from past and present, the community that is this department is something that has truly made my Bates experience something that I will continue to cherish after I leave here. From the long nights in Coram, to see kayaking during short term, the memories are endless.

Mom, Dad, and Allie, the continued love and support I receive from you is something I cannot appreciate enough. Not only have you embraced my adventures and spontaneous ideas, but you have always supported me as I try to figure out what my role and story will be. Without you three and the dogs, I could never imagine accomplishing the things I have and every day I am grateful to have you.

Thank You.

Contents

Contents

Introduction

Purpose and Significance

Over the past century, the global climate system has experienced unprecedented warming due to the rapid increase of greenhouse gas concentrations from human activity (IPPC, 2013). Due to the ongoing release of carbon dioxide (CO_2) to the atmosphere through the burning of fossil fuels, there has been increased attention warranted concerning global climate change. Since the role atmospheric CO_2 plays in the regulating global climate is well documented, understanding the fate of CO_2 once it is released is critical to evaluating the impacts of future climate change. Under conditions of changing climate, lakes have the potential to act as either a CO_2 sink, through the accumulation of organic matter in sediments, or a CO_2 source, through increased decomposition of organic matter.

As emissions of anthropogenic carbon dioxide continue to increase, understanding the complexities of the global carbon cycle become more critical. As a result, increased attention has been given to lakes as important actors in the global carbon cycle. Although lakes cover less than 2% of the Earth's surface, annual accumulation of organic carbon within lakes is equivalent to approximately 50% of the accumulation in all marine sediments (Dean and Gorham, 1998). This is despite the fact that oceans cover 71% of the Earth's surface, thus indicating that lakes may be important players in the carbon system. While displaying high overall rates of organic carbon accumulation, rates vary significantly different lakes due to differences in environmental factors controlling burial efficiency and accumulation (Kortelained et al., 2004). These factors, however, remain poorly understood and produce questions concerning the most important controls on burial efficiency and mass accumulation of organic carbon in lake sediments as well as the sensitivity of these rates to change over time.

Since sediments settle and accumulate at the bottom of lakes from the surrounding environments, they reflect the environmental conditions in which they were deposited, lakes provide proxies which produce detail records of environmental change. Analyses such as chlorophyll pigments can be used to develop an index of paleoproductivity and hence, summertime temperatures. In addition to recording changes in climate, lakes are important global reservoirs of organic carbon. Although many studies have examined modern carbon accumulation, paleo sequestration of carbon has received far less attention and warrants further investigation to determine how accumulation has varied and what controls exist.

The purpose of this study is to reconstruct the organic carbon accumulation contained in lacustrine sediments and to evaluate environmental and climatic controls on this process. Overall, this project will employ a multi-proxy approach and examine the sedimentary record from lakes spanning the boreal forest-tundra environmental gradient in the eastern Mealy Mountains, Labrador, Canada in order to: 1) help identify the most significant lake and watershed controls on organic carbon accumulation, 2) evaluate the sensitivity of organic matter accumulation to changing climatic conditions, and 3) constrain our understanding of past climate and environmental change in a region where very little prior information is available. A reconstruction of changes in organic carbon accumulation and environmental history was developed using sediment cores collected from the Mealy Mountains.

Lakes as Sentinels of Environmental Change

Given the vast and complex landscape of Earth's surface, questions emerge concerning how climate change influences ecosystems and the environment. Lakes and reservoirs are important in answering this question. Despite making up only a small percentage of the earth's surface, lakes act as sentinels by providing signals that reflect the influence climate change has on their much broader catchments (Williamson et al., 2009). Lakes comprise a large, geographically distributed network of ecosystems that can provide valuable information on both the patterns and the mechanisms of how terrestrial and aquatic ecosystems are responding to climate change (Williamson et al., 2009). As lakes produce physical, chemical, and biological responses, they are archived in their sediments, which enables paleolimnologists to investigate changes in climate over time (Figure 1). Sediments collected in lakes integrate these climate signals prior to deposition, while the accumulation of terrestrially derived carbon and outgassing of greenhouse gases make them hot spots of carbon cycling.

Solar radiation, air temperature, and precipitation are the primary mechanisms of climate forcing. Responses to such changes in lakes include physical (water level, water transparency, water temperature, thermal stratification, and ice cover thickness and duration), chemical (dissolved organic matter, oxygen, nutrient cycling), and biological (phenology, cold- vs. warm-water fisheries, clear water phase) characteristics (Figure 2; Williamson et al., 2009).

In addition to modern climate variations, lakes are considered to be integrators of past climate change as well. Lacustrine sediment archives integrate effects of climate variability on terrestrial and aquatic ecosystems through the deposition and preservation of diverse materials originating from terrestrial, aquatic, and atmospheric origins. Since lakes act as transformers of energy and mass inputs, which can be observed, lakes can provide information concerning changes in solar radiation, temperature, precipitation over varying time scales.

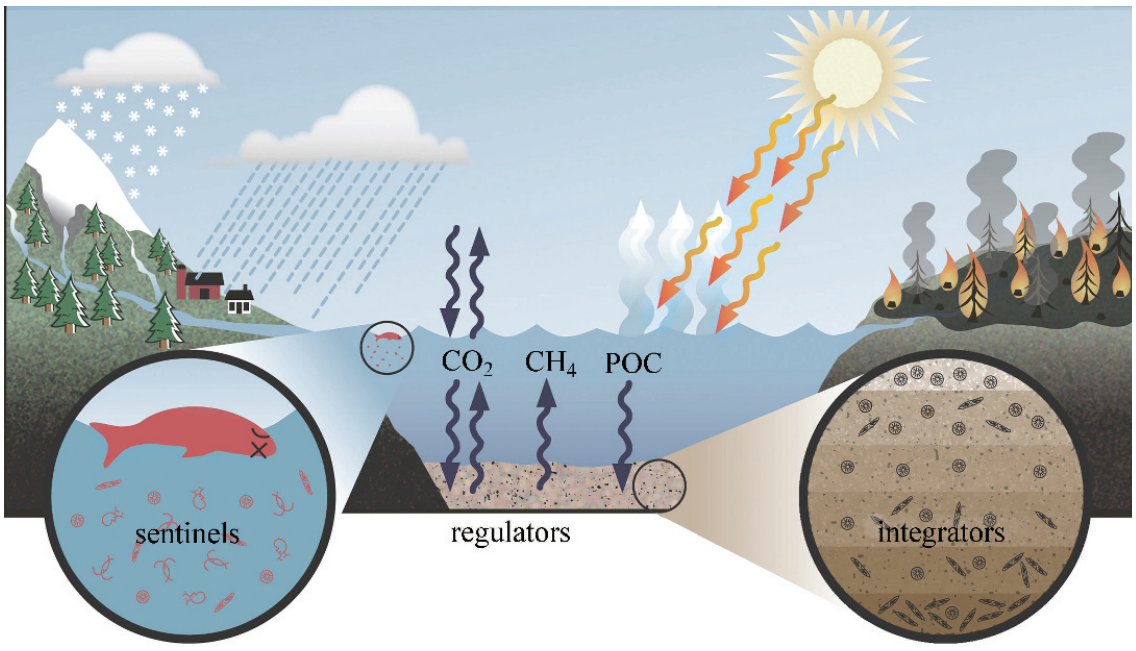

Figure 1. Conceptual model of lakes as sentinels, integrators, and regulators of climate change (from Williamson et al., 2009).

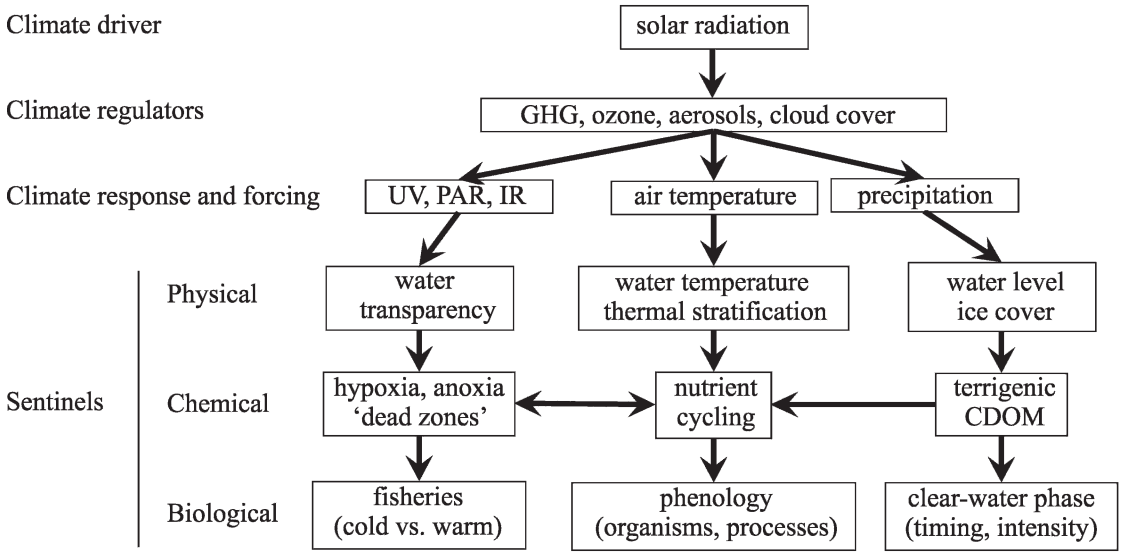

Figure 2. Flow diagram of lakes as sentinels of climate change, illustrating major climate regulators, climate response and forcing, and some physical, chemical, and biological sentinels that quantifiable (from Williamson et al., 2009).

Lakes as Carbon Reservoirs

In the biosphere, carbon is unevenly distributed throughout three major reservoirs: terrestrial, oceanic, and atmospheric. Traditionally, the global carbon cycle has been simplified and consisted of two biologically active boxes (oceans and lands) connected through gas exchange with a third actor, the atmosphere (Cole et al., 2007; Figure 7). Inland waters, however, receive and process large amounts of carbon derived from their watersheds and only half eventually reaches the sea (Cole et al., 2007). During this transport, there are two main potential sinks. The first, is through mineralization followed by evasion to the atmosphere, which occurs in rivers and lakes. The second, is through sequestration of carbon in lake sediments (Ferland et al., 2014). Inputs of organic carbon in lakes are deposited and collect at the bottom of lakes. As organic material accumulates, it will be either be mineralized to CO_2 or CH_4 by microbial activity or be buried in the sediment.

Despite receiving less attention than marine sediments, the storage of carbon in lacustrine sediments is recognized as a significant component of the total carbon budget. Although lakes cover less than 2% of the Earth's surface, annual accumulation of organic carbon in lakes is equivalent to approximately half of the carbon accumulated within marine setting (Dean and Gorham, 1998). Thus, suggesting lakes as carbon storage is important on regional as well as global scales (Ferland et al., 2013). Due to this increased interest in lacustrine storage of organic carbon, a search for predictors of carbon accumulation in lake sediments has been stimulated. Drivers such as lake area, lake dynamic ratio, as well as other catchment features have been identified, however, uncertainties remain concerning the pathways that lead to permanent carbon burial in lakes and the factors that control carbon accumulation rates.

Long-term carbon storage develops in four distinct stages. First, lakes are loaded with terrestrial organic carbon (OC), as both dissolved and particulate forms, and the synthesis of OC in the upper water layers. Second, this OC is delivered to the sediment through a downward particulate flux. Third, this OC is processed and degraded at the sediment-water interface and in the uppermost sediment layers. Fourth, OC continues to be removed in deeper sediment layers (Figure 3).

OC burial efficiency is the net result of the processing of sediment OC and represents that the proportion of sinking OC material that fails to be mineralized and is thus, permanently buried. The burial efficiency of OC is mostly dependent on factors affecting and regulating OC degradation, which include temperature (Gudasz et al., 2010) and oxygen exposure (Sobek et al., 2009). The origin of OC in lakes influences burial efficiency as well. Autochthonous production is preferentially degraded, while terrestrially derived OC is disproportionately accumulated (Gudasz et al., 2012).

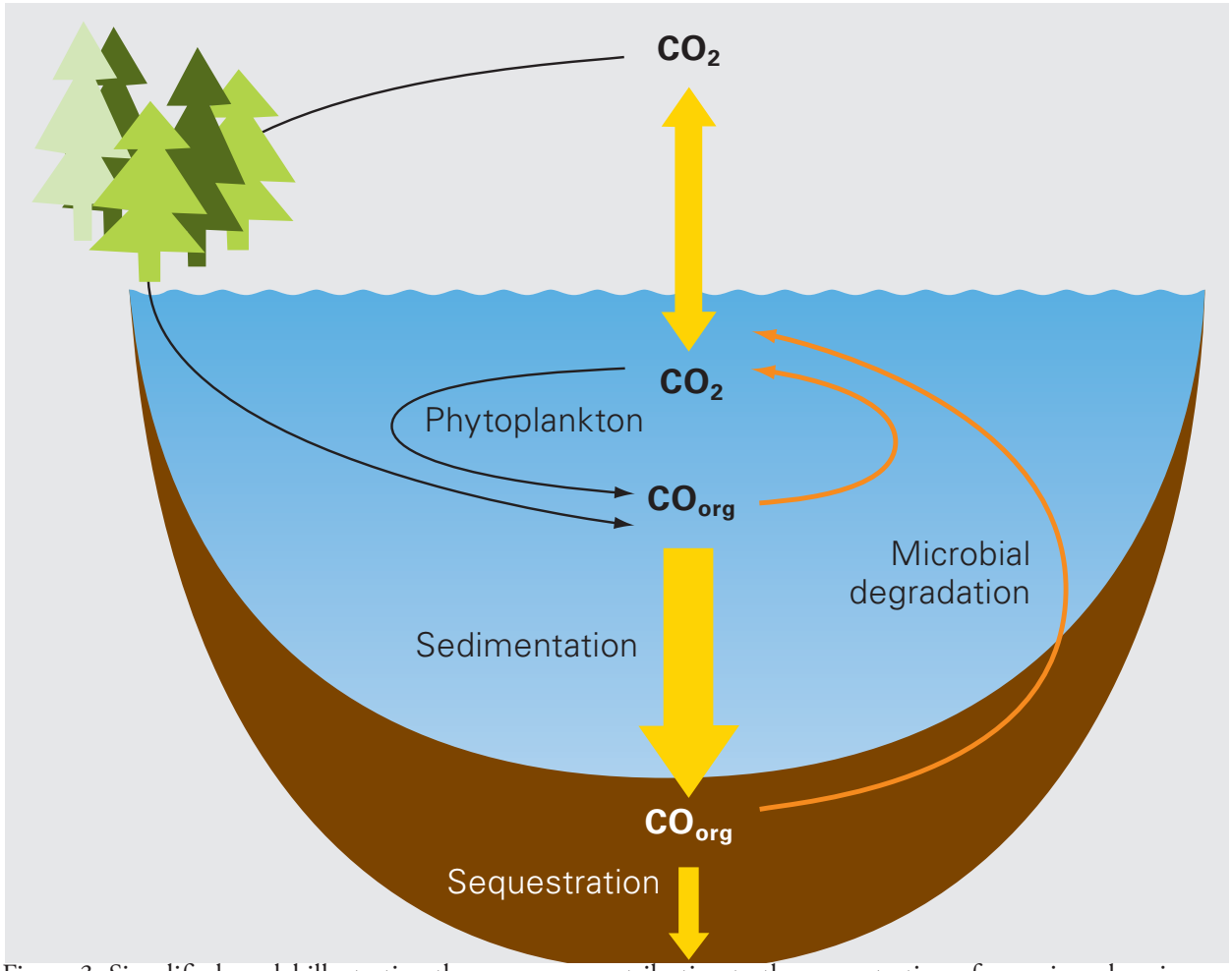

Figure 3. Simplified model illustrating the processes contributing to the sequestration of organic carbon in lake sediments. (From Sobek, 2009)

Setting

Newfoundland and Labrador

Newfoundland and Labrador is a Canadian province located in eastern Canada and extends 46°N and 60°N along the Labrador Sea (Figure 5). Central Labrador is characterized by a broad glaciated plateau that rises westward from the Labrador Sea that reaches elevations of more than 500 m above sea level. Narrow inlets dominate the coastal environment with Lake Melville, a 170 km long saltwater body, being the most prominent. Local bedrock geology is comprised primarily by granite and anorthosite (Wardle et al., 1997). The bioclimatic zones have been described as tundra, forest-

tundra, open woodland, and closed forest (Hare and Ritchie, 1972). The boundary between tundra and forest-tundra is defined by the northern most limits of scattered, coniferous trees, which are predominantly black spruce and white spruce (Picea glauca) (Figure X). This limit dips to the south from ca. 58.5° N at Ungava Bay to around 55° N over the northern Labrador Plateau before returning to the north at 58° N at the Labrador Sea (Hare and Ritchie, 1972).

Rising abruptly roughly 30 km form the south shore of Lake Melville and 100 km east-northeast from Happy Valley-Goosebay are the Mealy Mountains, which are a mountain range in the southern portion of Labrador that reach elevations of over 1100 meters above sea level and occupy an area of over 2000 km^2. The Mealy Mountains vary in topography and ecozones, which range from closed canopy forest to alpine tundra with bare summits and exposed bedrock. The mountains present a complex structural geology that has been heavily influenced by tectonic and erosional forces, which include the Quaternary glaciations, while lacking classic alpine glacial landforms. In addition, this study area experienced significant climate and environmental change during the past 10,000 years. Following the retreat of continental ice approximately 8,500 years ago (Occhietti et al., 2004), warm temperatures were experienced during the mid-Holocene and subsequent Neoglacial cooling that lasted into the 19th century.

Subarctic Glacial and Climate History during the Holocene

In terms of climate history, the Holocene climate record (11,500 cal yr BP) is marked by considerable variability, that includes retreating of continental ice sheets following the Last Glacial Maximum (LGM), changes in solar insolation, and shifting atmospheric circulation that have shaped many of the environemtns and landscapes studied today (Mayewski et al., 2004). One of the notable events that signifcantly impacted Newfoundland and Labrador was the presence and evenutal retreat of the Laurentide Ice Sheet (LIS) following the Last Glacial Maximum (Figure 4). As one of the three major domes of the LIS, the Labrador Sector covered an area of over 3,000,000 km^2 and probably reached a thickness of over 2 km during a period of low global sea level and relative climate stability (Dyke et al., 2002; Clark et al., 2000).

During deglaciation, ice flow was predominantly northeastward in central Labrador, eastward in the Lake Melville area, and southeastward in southeastern Labrador (Occietti et al., 2011). As the ice sheet retreated, Atlantic Ocean waters submerged glacioisostatically depressed coastal areas of central and southern Labrador, raising sea levels higher than the modern marine limit. In addition to causing rises in sea level, ice sheet retreat caused 1) a weakening of high pressure centered over the ice sheet and attendant changes in atmospheric circulation, 2) warming temperatures were caused

by the reduced heigh and extent of the ice sheet's albedo surface, and 3) a decrease in precipitaiton minus evaporation (Carlson et al., 2007) In Northern Quebec, the LIS lingered until about 6.8 ka and contributed a signifant influnece on the climate of this subregion long after adjacent areas had warmed (Kaufman et al., 2004).

During the first half of the present interglaciation, temperatures at high latitudes were generally higher, however, this warming occured at different times and to differnt degrees in different places (Kaufman et al., 2004). This spatio-temporal pattern of peak warming during the Holocene is known as the thermal maxiumum (HTM). On average, temperatures were 1.6°C higher than present. Alaska and northwest Canada experienced the HTM between 11 and 9 ka, which 4000 yr before the HTM in was displayed in northeast Canada. This dislayed warming in Quebec and Labrador is attributed to the resideual LIS, which caused cooler temperatures to persist (Kaufman et al., 2004)

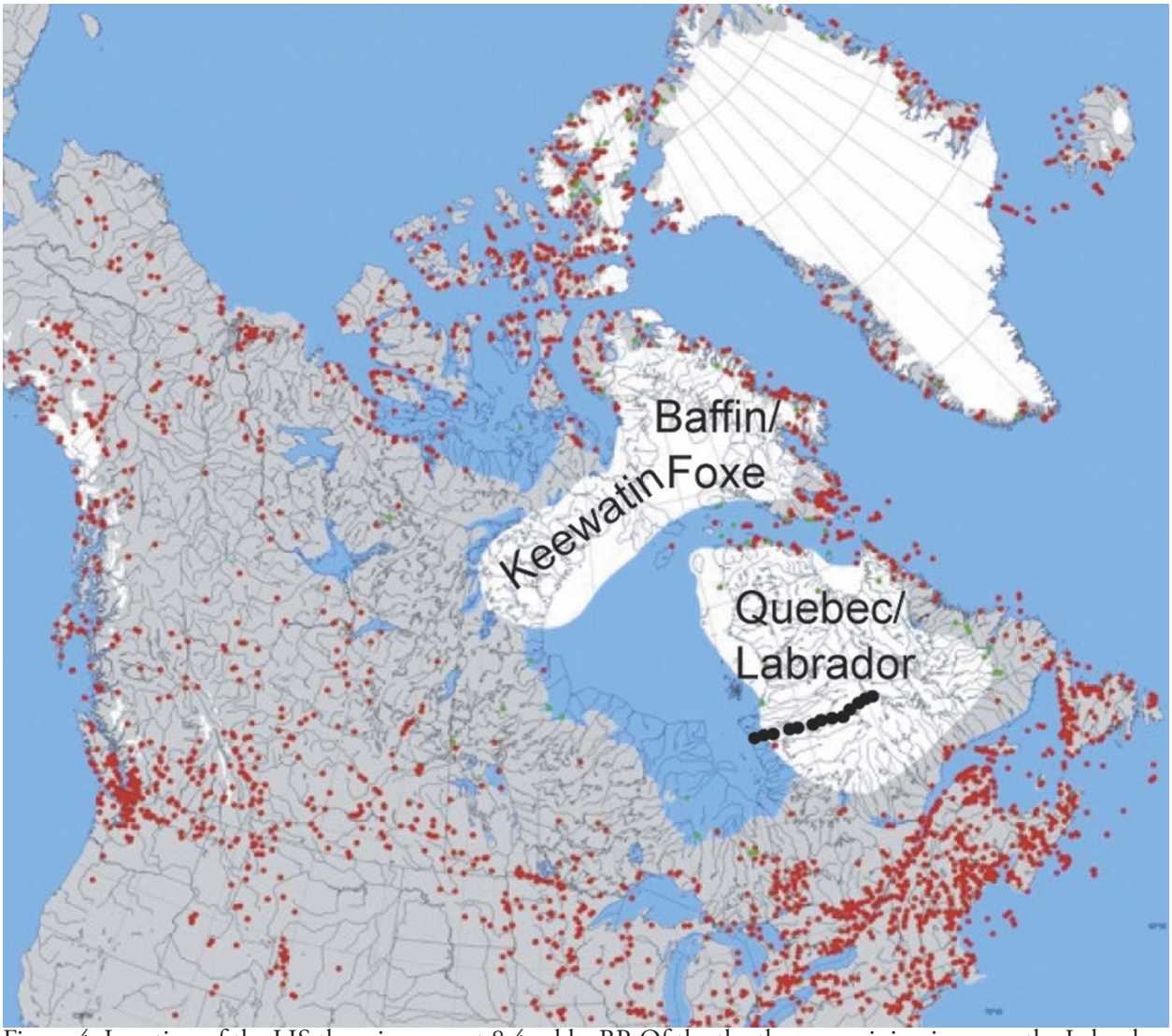

Figure 4. Location of the LIS three ice caps at 8.4 cal ka BP. Of the the three remaining ice caps, the Labrador sector was the largest. (From Carlson et al., 2007)

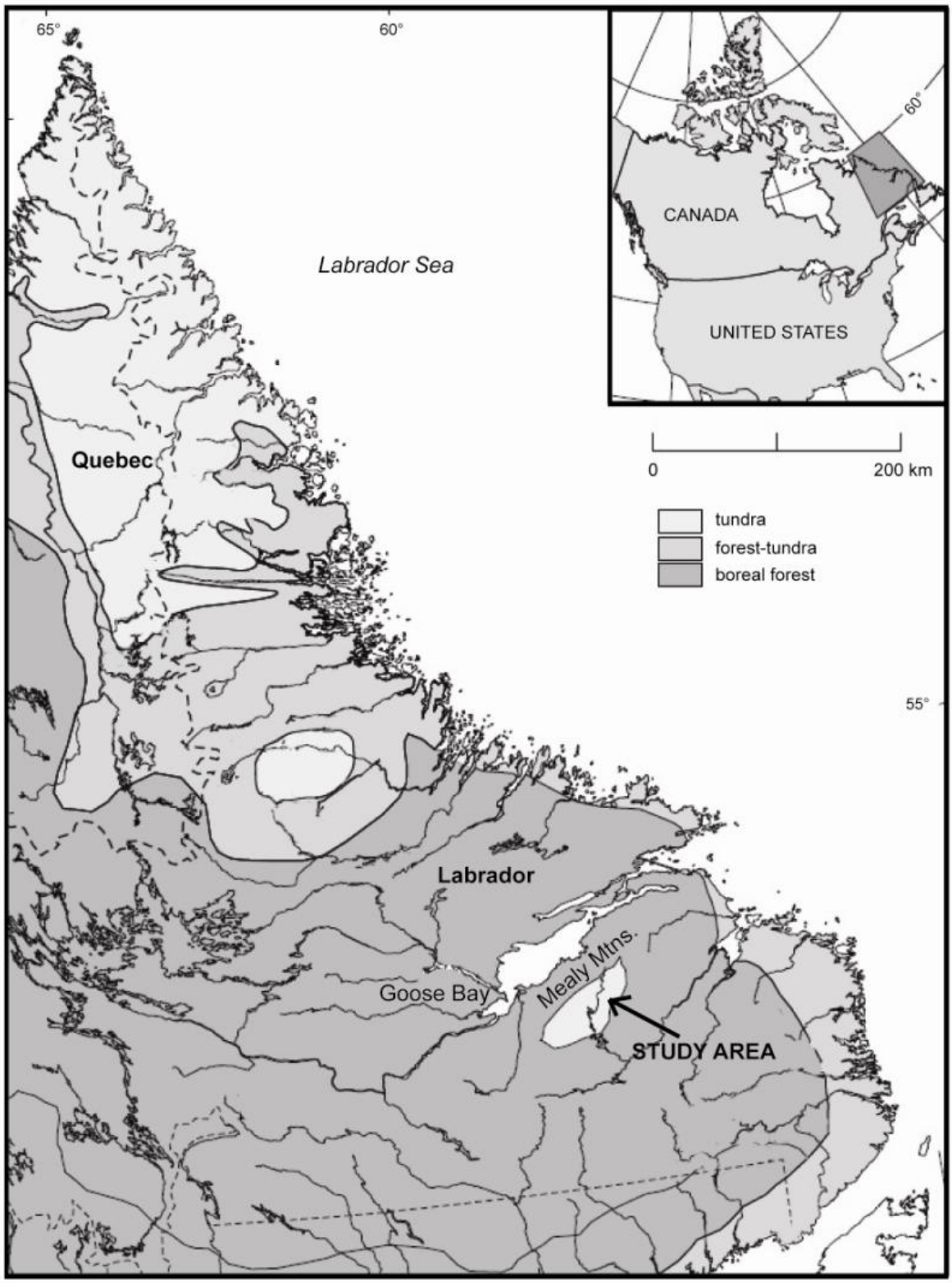

Figure 5. Regional map of Labrador. Dominant vegetation types are indicated as well as the study location within the Mealy Mountains. Notice that the study site is positioned along the tranistion between tundra and forest vegetation.

Regional Atmospheric Circulation

It is suggested that ocean circulation over the Newfoundland and Labrador Shelf and Slope display significant temporal and spatial variability (Han, 2005). The dominant flow features include the equatorward Labrador Current and the upper continental slope that carries colder and fresher water of Arctic origin, which subsequently has a direct influence on the shelf circulation (Loder et al., 1998). Additionally, the Gulf Stream and the North Atlantic Current interact directly with the Labrador Current along the Newfoundland Slope (Figure 6). Significant interannual variations in physical environments Labrador Current transport during the past decade (Han, 2005). Dramatic changes in biological productivity and fish stocks were experienced as well. It is proposed that these interannual variations are presumably are either directly or partially related by the dominant mode of atmospheric variability in the North Atlantic, which is the North Atlantic Oscillation (NAO). The NAO is defined as the sea level pressure difference between the Azores High and Icelandic Low (Hurrell, 1995).

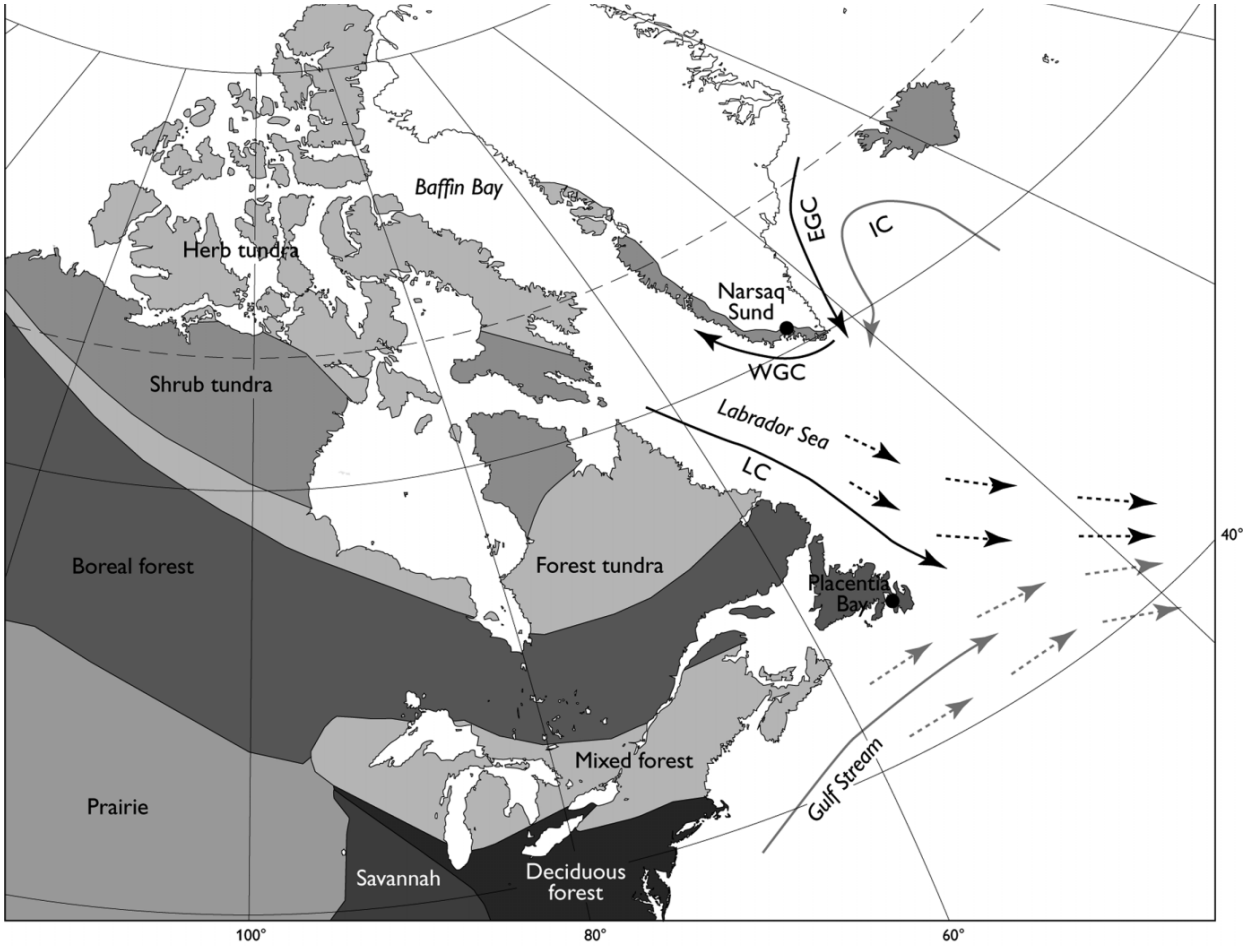

Figure 6. Map of the Labrador Sea region displaying the prominent forest/vegetation types as well as major oceanic currents. The Labrador Current (LC) brings cold water from the artic along the Labrador coast. (From Jessen et al., 2011).

Modern Labrador Climate

Due to the lack of earlier records, the regional instrumental record of climate in central Labrador begins ca. 1940 with meteorological stations established at Cartwright in 1936 and Goosebay 1941. The well documented Arctic warming during the mid-to-late 20th century did not initially include the eastern Canadian Arctic and Labrador (Jacobs, 2014). Instead a pronounced winter cooling occurred over northeastern Canada, including Labrador, from the mid-1970s through the early 1990s (Figure X; Banfield and Jacobs, 1998). By 2000, however, a warming trend in all seasons was underway in this region (Vose et al., 2005). Labrador temperature records display decadal-scale variability, like most of the North Atlantic, and are strongly related to the North Atlantic Oscillation and Arctic Oscillation (Jacobs, 2014).

Compared to the period from 1970 to 2000, summer time temperatures in central Labrador have increased by almost 1°C during the first decade of the 21st century (Environment Canada, 2011). It is predicted that this warming trend will continue and result in temperature increases of 3 to 4°C in the winter and 2 to 3°C in the summer by 2050 when compared to the period from 1970 to 2000 (Lemmen et al., 2008). Additionally, there has been a significant increase in annual precipitation in Labrador over the 20th century and was accompanied by an increase in the rain-to-snow ratio (Zhang et al., 2000).

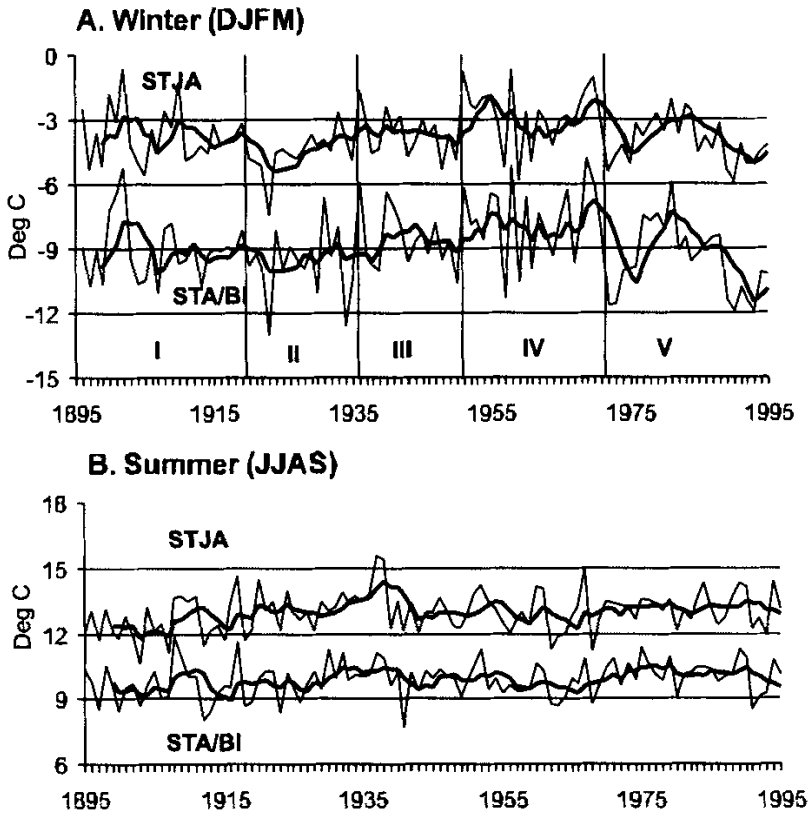

Figure 7. Intrumental temperature record for modern Labrador climate. (From Banfield and Jacobs, 1998)

Local Glacial and Climate History

Two continental glaciation (Wisconsin in age) have been noted in the eastern Mealy Mountains (Gray, 1969). The older ice sheet reached a minimum elevation of 3,000 feet and may have overtopped many of the summit plateaus of 4,000 feet. Ice flowed from west to east. The later ice sheet varied in height from 2,300 feet in the west to 1,800 feet in the east. Both glaciations displayed evidence of carving from glacial cirques. Development of active glaciers with pronounced end moraines, subsequent to the later glaciation was restricted to cirques oriented towards the east and southeast. Cirque re-advancements have probably not occurred within the last few hundred years.

Bedrock Geology

The southeast Mealy Mountains is located in the Grenville Province in eastern Labrador (Figure 8). The northwest part of this region consists of barren or sparsely vegetated upland to mountainous region. This forms the southeastern flank of the mountain chain. Many of these hill exceed 600 m elevation and the highest point is over 820 m. The topography in the upland area is controlled by east-northeast and north-northwest trending fracture sets (Gower and van Nostrand, 1996). These are most prominent in northern and westernmost districts. The region grades into lower, wooded hills to the south and east. The highest areas coincide with monzonitic bedrock of the Mealy Mountains Intrusive Suite.

This study area was located in the northeastern Grenville Province and straddles the boundary between the Exterior Thrust and Interior Magmatic Belt, which includes the Mealy Mountains terrane (James and Nadeau, 2001). The Mealy Mountain terrane consists mostly of Late Paleoproterozoic plutons of the Mealy Mountain intrusive suite (MMIS), minor amounts of Paleoproterozoic pre-Labradorian crust, and Pinwarian and late- to post-Grenville intrusions (Gower, 1996). Generally, the Mealy Mountain terrane includes variably of recrystallized, deformed and locally gneissic, granite, monzonite, monzodiorite, syenite, and grabbro. The MMIS is composed of an older group of anorthositic, leucogabbroic and leucotroctolitic rocks and a younger group of pyroxene-bearing monzonite and quarts bearing monzonite intrusions (James and Nadeau, 2001).

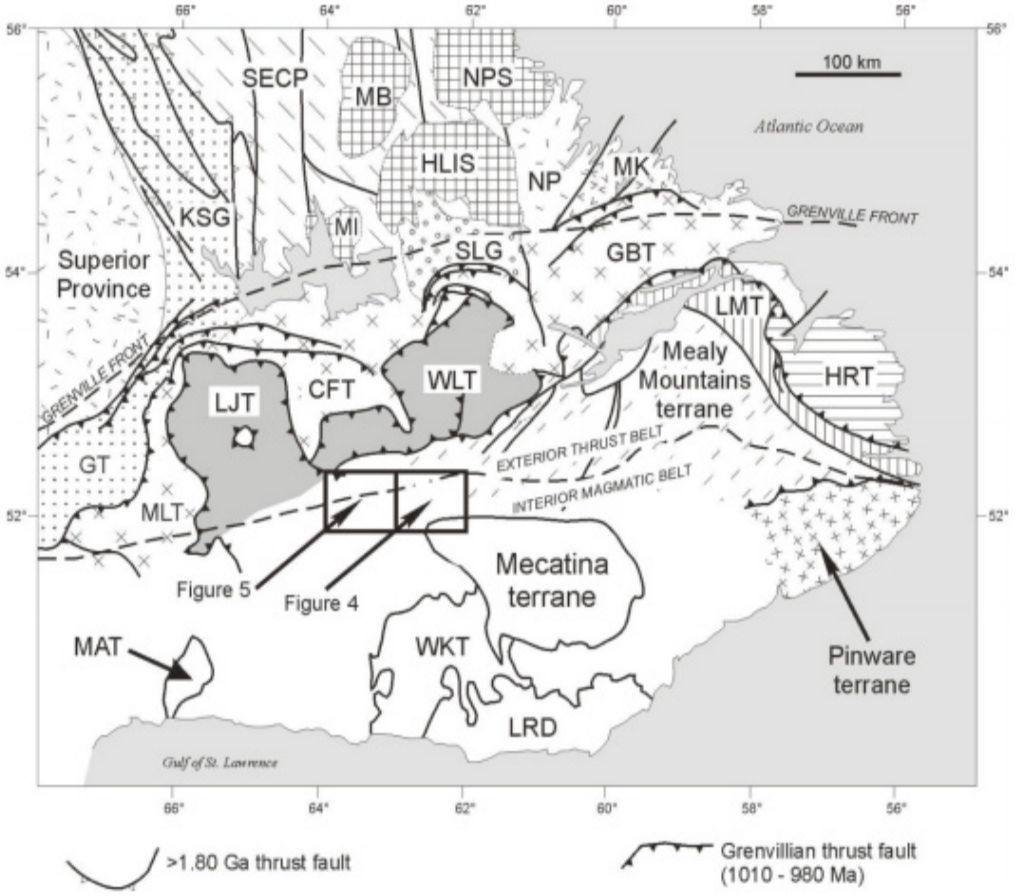

Figure 8. Tectonic setting and major lithotectonic units of southern Labrador. Study site is located within the Mealy Mountains terrane. (From James and Nadeau, 2001)

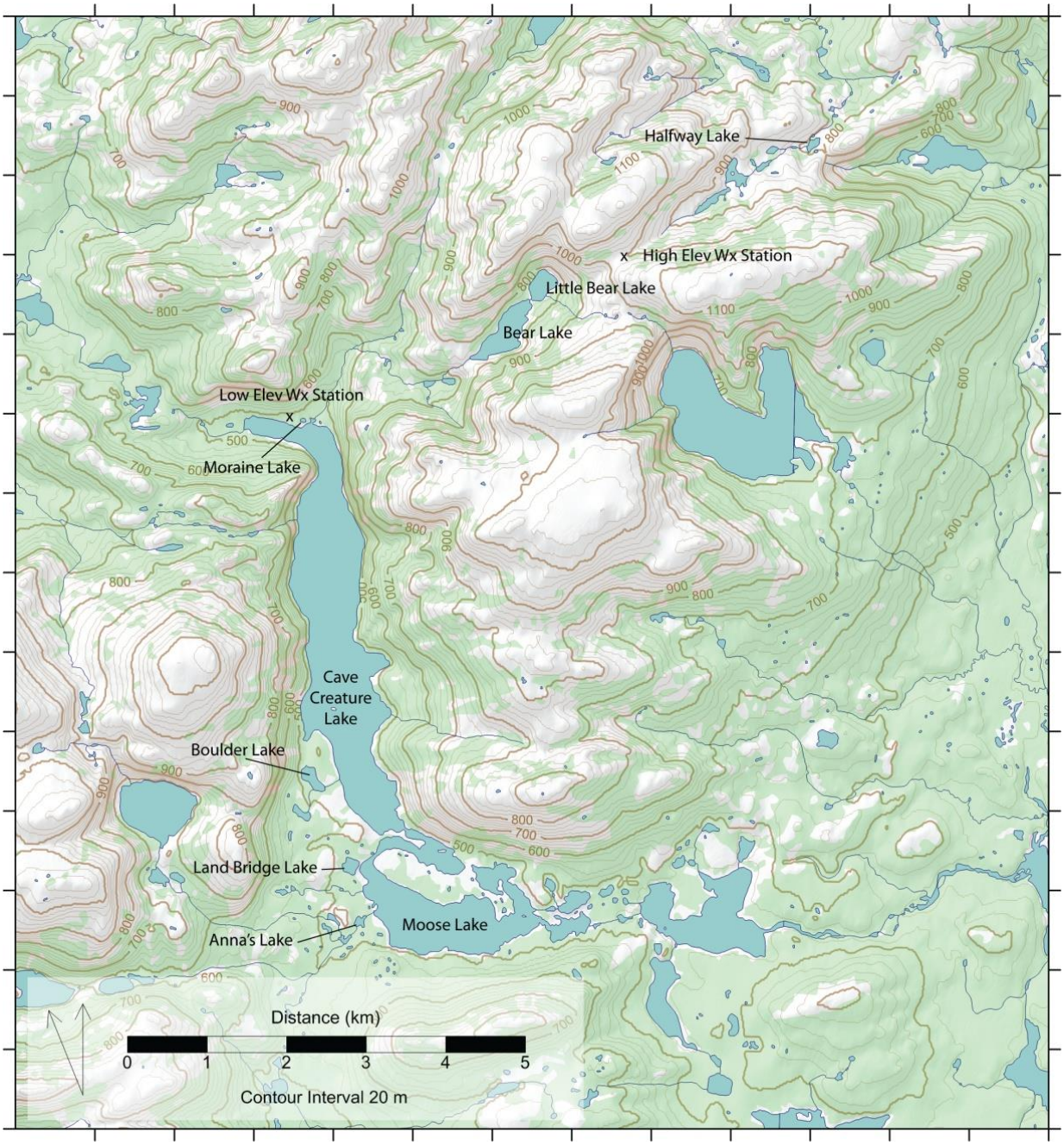

Figure 9. Map of the study area surrounding Moose Lake. To the north of the studied lake are areas of higher elevation with steep peaks. To the south is mostly forest-tundra vegetation.

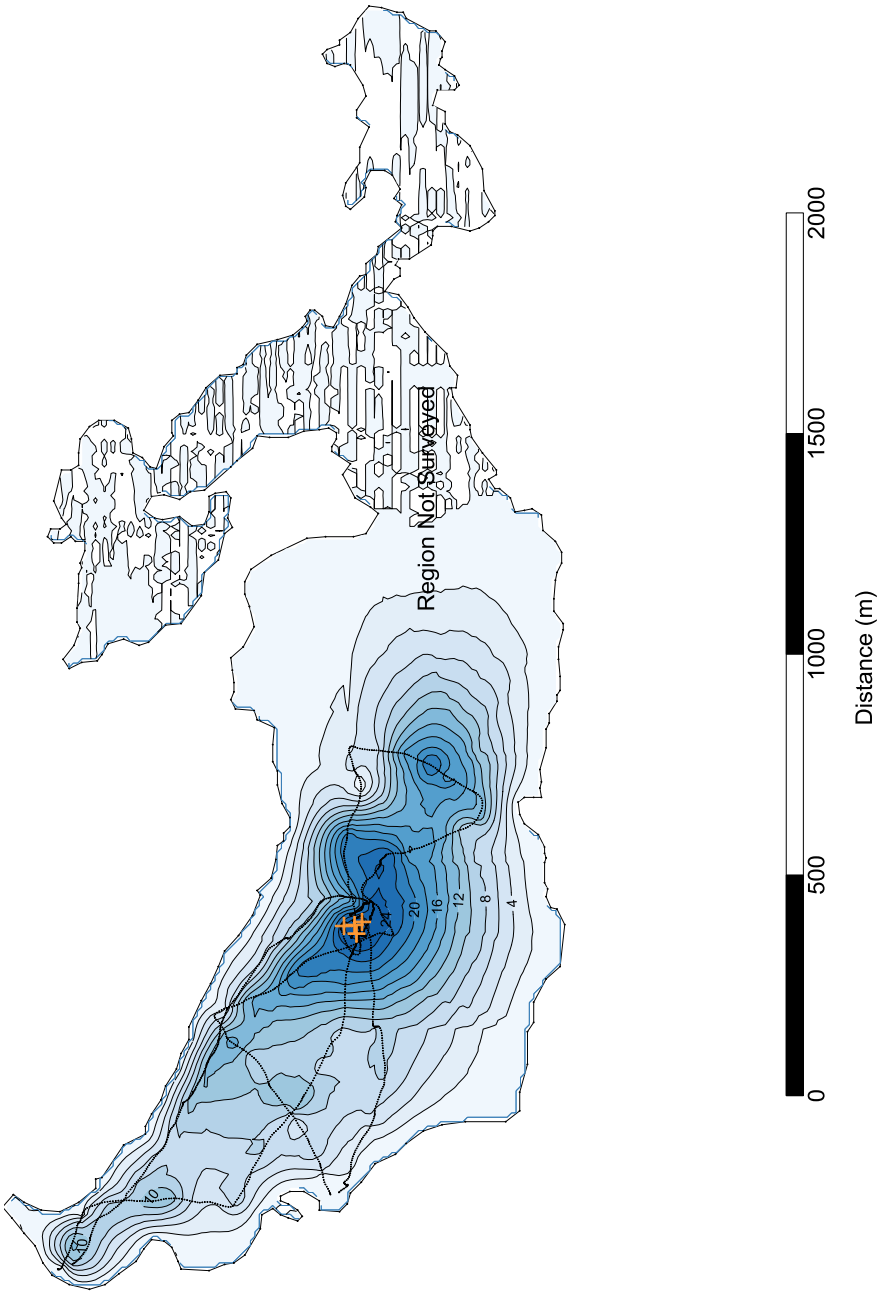

Figure 10. Bathymetric map of Moose Lake. Transects made are indicated by black lines. Coring site is located in the deepest part of the lake and indicated in orange. (Map made by Dr. Timothy Cook)

Study Site

The specific study area is located along the eastern margin of Mealy Mountains in southeastern Labrador at 53.5786° N, 58.5896° W (Figure 9). Based on this location, the Mealy Mountains fall squarely within the latitudinal belt (40-60°N) in which the majority of modern lakes are found (Talbot and Kelts, 1989). The glacially scoured and shaped area hosts a high concentration of lakes that vary in size and shape. This includes many lakes that are rather deep relative to their overall size (Lamb, 1984). Of these lakes, Moose Lake is 1.85 km^2 in size and is located at an elevation of 484 m a.s.l. (Figure 10). The catchment area of Moose Lake is 7.477 km^2 and has a maximum watershed elevation of 929 m a.s.l. The maximum depth is 27 m.

Summary:

Over the past century, the global climate system has experienced unprecedented warming due to the rapid increase of greenhouse gas concentrations. Thus, understanding the fate of CO_2 once it is released is critical to evaluating the impacts of future climate change. Lake sediments have the potential to store large quantities of CO_2 in the form of organic carbon, yet the factors which control organic carbon burial efficiency in lakes are not fully understood. Consequently, this project examines the sedimentary record from one lakes positioned along the boreal forest-tundra ecotone in the eastern Mealy Mountains of southeastern Labrador, Canada in order to identify lake controls on organic carbon accumulation and to evaluate the sensitivity of organic matter accumulation to changing climatic conditions. The pronounced environmental gradient and significant post-glacial environmental changes in this region provide an ideal setting for testing controls on organic matter accumulation.

Methods

Field Methods

All fieldwork was conducted during the field campaign, which was held from July 18 through August 11 in the eastern Mealy Mountains of southeastern Labrador, Canada. The study area was accessed via float plane from Goose Bay, Labrador which in turn was reached via Trans-Labrador Highway.

Bathymetry

The bathymetry of each lake was determined using a Lowrance mapping GPS w/ echo sounder and sidescan sonar attached to small inflatable rowboats. Several transects across each lake were completed to accurately construct the bathymetry of each. Bathymetric profiles were used to define lake morphometry and to determine suitable coring sites, which were identified as the basin(s) within each lake, since these are areas of maximum sediment accumulation within a lake. Bathymetric maps were generated using Surfer 12 by Timothy Cook after returning from the field investigation.

Water Column Properties

Water column profiles were completed for each lake. Temperature and specific conductivity profiles within the water column were created using a YSI conductivity-temperature-depth probe. Dissolved oxygen profiles were generated by collecting water samples at various depths using a van dorn water sampler and then measured using a YSI ProODO handheld Dissolved Oxygen meter. Secchi disk and meter line were used to measure the transparency of the water, which reflects water turbidity. Water pH values were measured using a field pH sensor.

Sediment Coring

One sediment core (1.43 m) was collected from Moose Lake (14-2-2) n August 4th, 2015. The core was obtained using modified weighted, percussion-percussion corer with a flapper valve mechanisms and triggered by metal messenger. Sediment was collected in clear plastic tubing with an interior diameter of 6.6 cm and that utilized one-way valves. This was to ensure that sediment was disturbed or lost as the core was pulled up through the water column after the coring process was completed. A piston-percussion corer was used to collect core MM08 in order to collect a longer core. The core was pulled up by hand and capped below the surface of the water. Floral foam was inserted at the top and bottom of the core to ensure sediment was securely packed for transport to the University of Massachusetts in Amherst, Massachusetts.

Laboratory Methods

Cores were split using a Geotek core-splitter at the Hartshorn Quaternary Lab at the University of Massachusetts, Amherst. The core splitter uses a combination of vibratory cutters and hooked slitting blades to cut the plastic core tubing. A stainless steel wire was then used to cleanly split the sediment. One half was archived and stored in the UMass, Amherst core room and the other half was used for both non-destructive analyses and subsampling-based analyses. When not being analyzed, cores were

wrapped in plastic, stored horizontally, and refrigerated.

Non-Destructive Analysis

A visual stratigraphic log was made for core ML-14-2. Qualitative sediment characteristics (color, texture, composition, and structure) were used to describe the visual stratigraphy. All quantitative non-destructive analyses were completed at the Hartshorne Quaternary Lab at UMass, Amherst.

Geotek Core Logger

Each of the three sediment cores were processed using a Geotek Core Logger, which was used to obtain high-resolution, down-core data that included gamma density, magnetic susceptibility, color spectrometry, and line-scan imagery at 0.5 cm intervals. Gamma density provides a precise and high resolution record of bulk density, which can be used as an indicator of lithology and porosity changes, by measuring the number of transmitted gamma photons that pass through the core unattenuated. Magnetic susceptibility correlates with variations in the sedimentary provenance and is measured by the degree of magnetization that a sediment experiences when subject to a magnetic field. Color spectrometry produced quantitative information concerning sediment color by measuring reflectance, which helps remove subjectivity in sediment color assessment. A high resolution images were produced for each core using the line-scan imaging capabilities of the Geotek Core Logger.

ITRAX Core Scanner

Core ML-14-2 was analyzed using a Cox Analytical Systems Core scanner at the UMass Geosciences X-Ray Fluorescence Lab. Plastic wrapping was removed from each core in order to perform the surface optical scan. Using the X-radiographic capabilities, a high resolution density scan of each core was produced. X-ray fluorescence (XRF) was collected in counts per second at 1 mm intervals, while the X-radiographic signal was set from 3500-8000 milliseconds. XRF analysis was conducted for 50 elements including Fe, Rb, Ti, Mn, Ca, K, and Sr. Correlations were determined between the different elements by creating correlation matrices.

Radiocarbon Dating

Seven samples of organic macrofossils were collected from throughout the core at varying depths and sent away to DirectAMS in Seattle, Washington. Samples were measured by accelerator mass spectrometry (AMS) radiocarbon age dating. Samples were a mix of leaves and wood fragments found at cumulative depths of 25 cm in MM01 and 107.5 cm in MM08. The ages returned by DirectAMS were already calibrated and calculated 1sigma error.

Destructive Analysis

Bulk Density and % LOI

Carbon analyses were conducted using 1 cm3 of sediment sampled from the core at 1 cm resolution. Samples were removed using a modified cut-off medical syringe. At each interval, precisely 1 cm3 of sediment was placed into a pre-weighed crucible. All mass measurements were measured to 0.0001 mg. After weighing the wet bulk density, samples were dried at 1000°C for 16 hours. Samples were

weighed again to determine dry bulk density and the incinerated in a Thermolyne 6000 muffle furnace at a constant temperature of 550°C for four hours. The final masses of the crucibles were then measured and used to determine % water content and % Loss on Ignition using the following equations:

Wet Bulk Density = (crucible + wet mass - crucible mass)/ 1 cc

Dry Bulk Density = (crucible + dry mass - crucible mass)/ 1 cc

% Water Content = ((wet mass - dry mass)/(wet mass)) * 100

% LOI = ((dry mass - burnt mass)/(dry mass)) * 100

Carbon, Nitrogen, and Stable Isotopes

Subsampling of core ML-14-2 for % C, % N, C/N and stable isotopes was performed at 2 cm intervals for the top 10 cm of the core (0-10 cm) and then at 2 cm intervals for the rest of the core. Approximately 1 cm^3 of sediment was sampled and then freeze dried. Between 3-6 milligrams of each 1 cm^3 were measured out on a microbalance in 5 X 9 mm tin cups. Samples were analyzed using a Costic 4010 Elemental Analyzer (EA) interfaced via combustion to a Delta V Advantage Isotope Ratio Mass Spectrometer (EA-C-IRMS) in the Bares College Environmental Geochemistry Lab. Three sets of standards (blank tin cup, acetanilide, and caffeine) were run at three different times (beginning, interspersed, and end) in order to correct for uncertainty. C/N ratios were calculated from total organic carbon and total nitrogen.

Chlorophyll Analysis

Chlorophyll pigment analysis provides a proxy for paleoproductivity and summertime temperature. The abundance of chlorophyll-a pigments reflects the amount of active algal biomass in a sample. Over long term sediment records, chlorophyll-a degrades into various phaeopigments (Taguchi et al., 1993). Thus, requiring both to be analyzed in order to create the paleoproductivity of a lake contained in the sediment record. Since chlorophyll fluoresces colors within the red part of the color spectrum when subject to light at blue wavelengths, it possible to calculate the concentrations of both chlorophyll-a and its degradation products.

Total chlorophyll pigments were determined from 1 cm3 sediment samples at 2 cm intervals. 10 mL of a 90% acetone solution were added to each sample in centrifuge tubes and sonicated for 30 seconds using a Branson Sonicator. Samples were capped and stored in a dark freezer. After 12-20 hours, samples were thawed and then centrifuged for 5 minutes at 2.5. 1 mL of supernatant was pipetted into a cuvette, followed by 9 mL of 90% acetone. Samples were inverted to mix and then run through a Turner Designs 10 AU fluorometer. The abundance reading of each sample was recorded (at what wavelength?). Samples were then acidified with 3 drops of 6M HCL, mixed, and processed through the fluorometer. Samples were acidified in order to degrade active pigments to phaeopigments. This enables the total chlorophyll pigment calculation can be divided between active chlorophyll pigments and inactive, phaeopigments.

Results

Core Description

Visual Stratigraphy

The sediment sequence from Moose Lake (ML-14-2) is comprised of three distinct lithostratigraphic units: A, B, and C (Figure 11). The top later (Unit A) is predominately a homogenous dark brown/ black, organic rich gyttja (0-102.5 cm). At the very top of this unit (2 cm), a thin red layer is observed followed by a 1 cm thick gray layer. Underlying this unit is a slight gray transition layer (Unit B) that is densely concentrated with organic macrofossils (102.5-111.5 cm). Unit B is composed of a combination of both organic and inorganic rich sediments. A sharp transition is observed at 111.5 cm at which becomes predominantly clastic in nature with very little organic matter visible and continues through the bottom of the core (Unit C). At 129.5 cm the sediment transitions form a yellowish-brown into a dark gray, clastic dominant silty-clay. The very bottom of this unit was disturbed during the coring process, but the bottom 4 cm were preserved and is characterized as a silty or fine sand based on a qualitative grain size estimate.

Reflectance Spectroscopy

L* (lightness parameter) ranged from 19.19% to 40.84% (Figure 12). L* (darker color) values are displayed throughout unit A, with higher (lighter color) values in unit B, and the highest (lightest color) values in unit C. A* values were highly variable and ranged from -2.81 to 2.26. The highest a* (red) values were observed from 0 to approximately 100 cm. The lowest (green) values were seen at the bottom of the core. Parameter b* ranged from 2.64 to 11.01 and displayed more variability than the other two parameters (mean = 5.91 ± 1.38).

Magnetic Susceptibility

Magnetic susceptibility measurements were made at 0.5 cm increments along core ML-14-2-1 and ML-14-2, which are displayed in Figure 12. Changes observed in the measured magnetic susceptibility correlate well with the observed three lithostratigraphic units described. Values were lower through unit A and begun increasing in unit B. Unit C displayed the highest measurements found in the entire core, with highest values occurring from 130-138.5 cm.

Due to the high values found at the bottom of the core, variations in magnetic susceptibility in unit A are not displayed To correct for this, Figure 16 was constructed as a higher resolution representation of the finite changes in sedimentary provenance of the uppermost unit. The highest values found in unit A are found in the ranges from 0-4 cm and 102-105 cm, which include the two highest values recorded (1 cm and 103.5 cm). A small peak is shown at 21.5 cm followed by consistent measurements until 83.0 cm where oscillating fluctuations are observed that continue into unit B with greater amplitudes.

Unit A:
Homogenous
darkbrown/black
organic gyttja

Unit A:
Homogenous
darkbrown/
black organic
gyttja

Unit B: gray
transition layer
(mix of organic
and inorganic
material)

Unit C: Dark
grayish brown
transition into a
dark gray clastic
dominant clay

Figure 11. High resolution image of core ML-14-2 collected from Moose Lake taken by the Geotek core logger. Core desciptions are prented to the left. The 139.5 cm long core was split into three different lithostratigraphic units based on visual properties and characteristics.

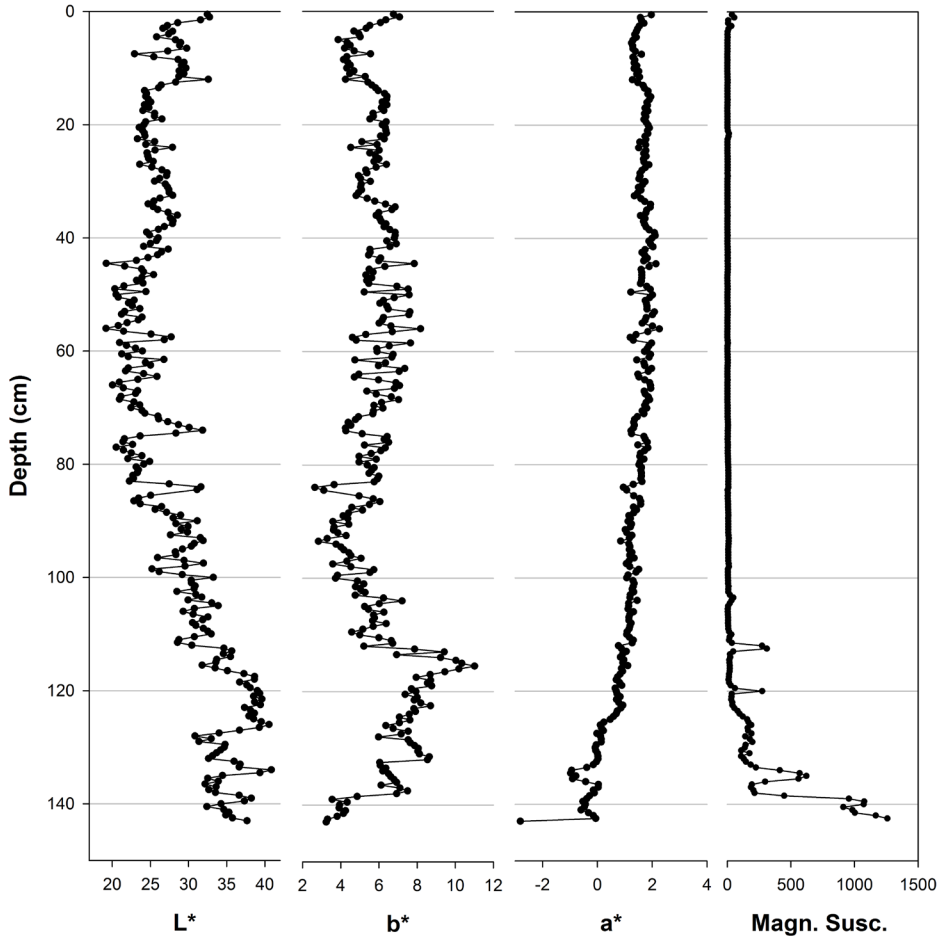

Figure 12. On the left, down core profiles of relectance spectroscopy (L*, a*, and b*). Right, magnetic susceptibility profile.

Sample ID	Sample Description	Cumulative Depth (cm)	Delta 13C (per mil)	Radiocarbon Age BP	1sig error	Calibrated Age Ranges	Midpoint Age (Cal BP)
Mealy-003	Plant Fragments	7.5	-18.1	1604	24	1473 - 1549	1511
Mealy-004	Plant Fragments	15.5	-22.5	1543	25	1380 - 1523	1451.5
Mealy-005	Plant Fragments	35.5	-18.7	2247	26	2157 - 2262	2209.5
Mealy-006	Plant Fragments	49.5	-15	2343	27	2324 - 2435	2379.5
Mealy-007	Plant Fragments	76	-25	3588	69	3703 - 4014	3858.5
Mealy-008	Plant Fragments	93	-23.8	4142	28	4575 - 4773	4674
Mealy-002	Plant Fragments	107.5	-31.2	5022	27	5806 - 5891	5848.5

Table 1. Summary of returned AMS ^{14}C radiocarbon dates for organic macrofossils collected from various depths throughout the core.

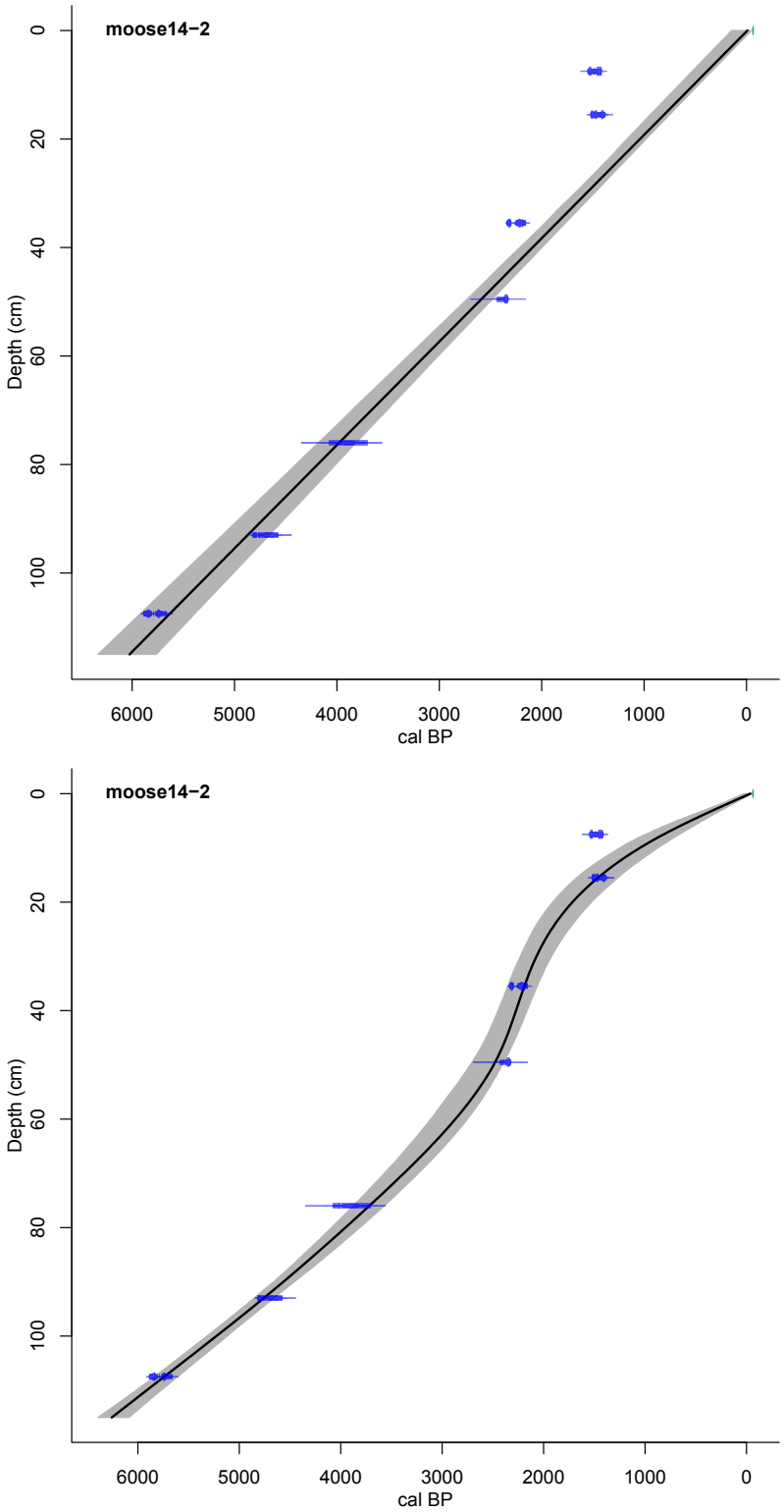

Figure 14. Age-depth models for core ML-14-2, based on seven ^{14}C ages calibrated to cal yr BP. The top model, was constructed using a linear regression, while the bottom model is based on a smooth spline relationship between points. Based on both models, the record archived in core ML-14-2 covers at least ca. 6000 cal yr BP.

Age Model

AMS ^{14}C Radiocarbon Dating and Calibration

A total of seven organic macrofossils from different depths throughout the core were collected for radiocarbon dating. All samples were analyzed and dated by DirectAMS in Seattle, Washington for ^{14}C age measurements using accelerator mass spectroscopy (AMS). Table 1 presents the age estimates in ^{14}C years and associated one-sigma calculated error. The radiocarbon ages display a fairly linear trend through the early and middle portions of the record, however, towards the top of the record there is an age reversal from 1543 ^{14}C years BP to 1604 ^{14}C years BP. The generated radiocarbon ages were calibrated into a calendar years BP time-scale using Clam 2.2., which utilizes the northern hemisphere terrestrial calibration curve IntCal13. ^{14}C from Reimer et al. (2013).

Age-Depth Modeling

Having established the calibrated ages for individual core levels, extrapolating the age estimates for all depths in the core is required. The calibrated age estimates (cal BP) that were calculated based on the radiocarbon ages, were processed semi-automatically in order to obtain age-depth models for the sedimentary record. Two age models were constructed: Figure 14a was constructed based on a linear regression through all points and Figure 14b is based on a smooth spline curve. The linear regression based model assumes that there is no net change in accumulation rates over the entire record and avoids the upper three radiocarbon samples suggesting that there are anomalously old. In contrast, the smooth spline curve based model displays variation in sedimentation rates and avoids only the upper most sample in order to account for the age reversal found at the top of the record. This model differs from the linear regression model in the middle portion as it requires that there be a significant increase in accumulation rate at approximately 2500 cal yrs BP followed by a subsequent decrease in accumulation rate at 2000 cal yrs BP. Each model was only extrapolated down to 115 cm depth because no geochronological information was obtained below the transition to a more clastic sediment.

Geochemical Analysis

Elemental Profiles

Elemental data produced by the Itrax Core Logger is recorded in terms of counts per second (cps) rather than absolute concentrations, but can be used to observe relative changes in the elemental profiles in contrast to absolute concentrations. Down core profiles of the elements used in this study (Fe, K, Ca, Ti, Mn, Rb, and Sr) are displayed in Figure 15. Through unit A (0-102.5 cm), counts per second values remained relatively low for all elements. K, Ca, and Mn exhibited slight increases with depth. After displaying relatively fixed values, large and abrupt peaks were observed around 102.5 cm and 108.5 cm in the K, Ca, Ti, Sr, Mn, and Fe profiles. Following these increases, cps values for all elements increased significantly through unit C, where the highest concentrations for each element were displayed.

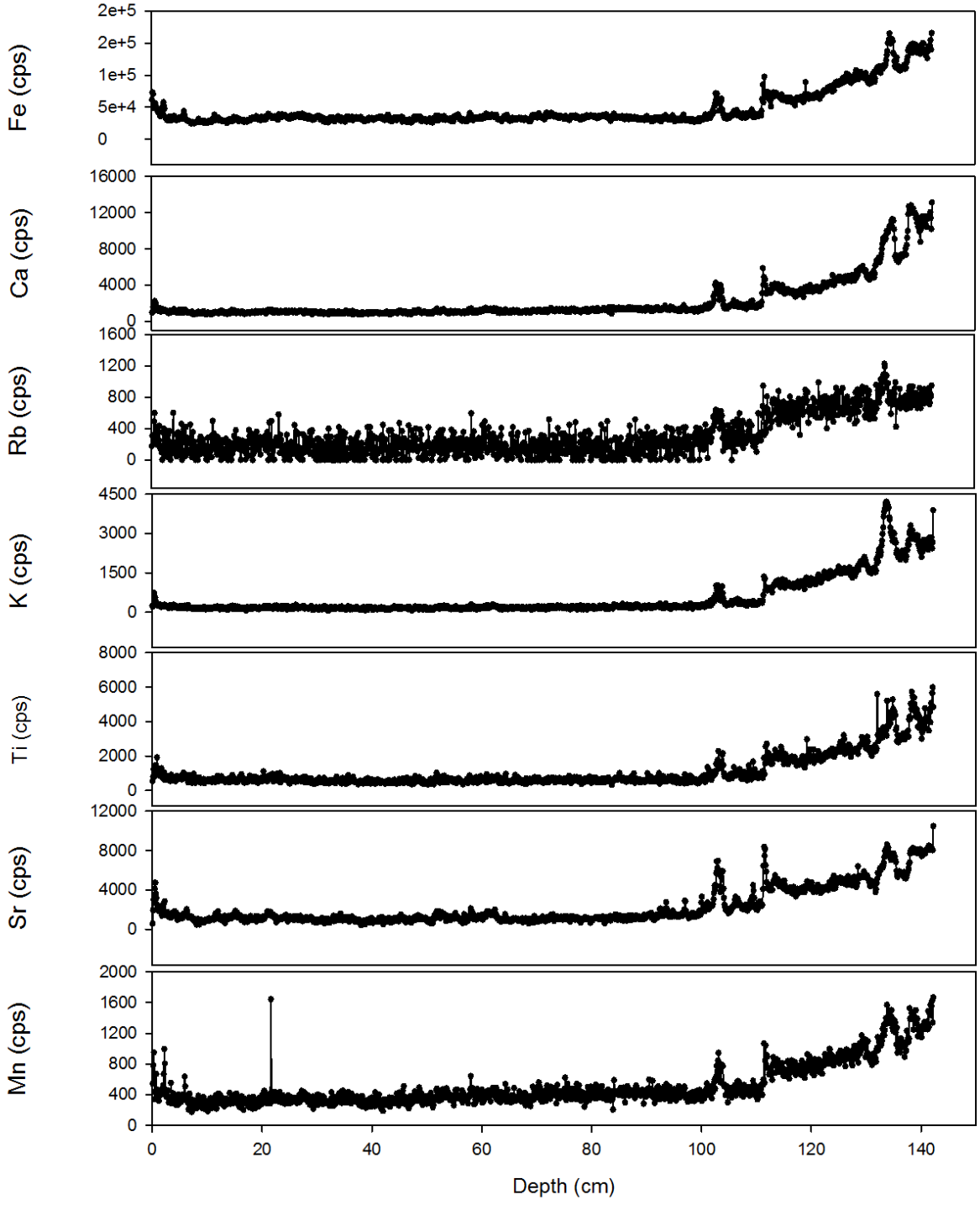

Figure 15. Down core profiles of Mn, Sr, Ti, K, Rb, Ca, and Fe in counts per second (cps). Each profile is plotted against depth. Highest cps values are shown from 102.5 cm depth to the bottom of the core.

	Si	K	Ca	Ti	Mn	Fe	Rb	Sr
Si	1							
K	0.920958	1						
Ca	0.833035	0.963929	1					
Ti	0.848499	0.956739	0.969097	1				
Mn	0.857856	0.944654	0.941054	0.945252	1			
Fe	0.855331	0.965664	0.974633	0.973078	0.958087	1		
Rb	0.794372	0.844719	0.795761	0.823027	0.826135	0.822728	1	
Sr	0.830703	0.938846	0.937184	0.940031	0.939051	0.942638	0.867436	1

Table 2. Correlation matrices indicating the degree of associateion between the elements examined in this study, Most pairs display strong correlations.

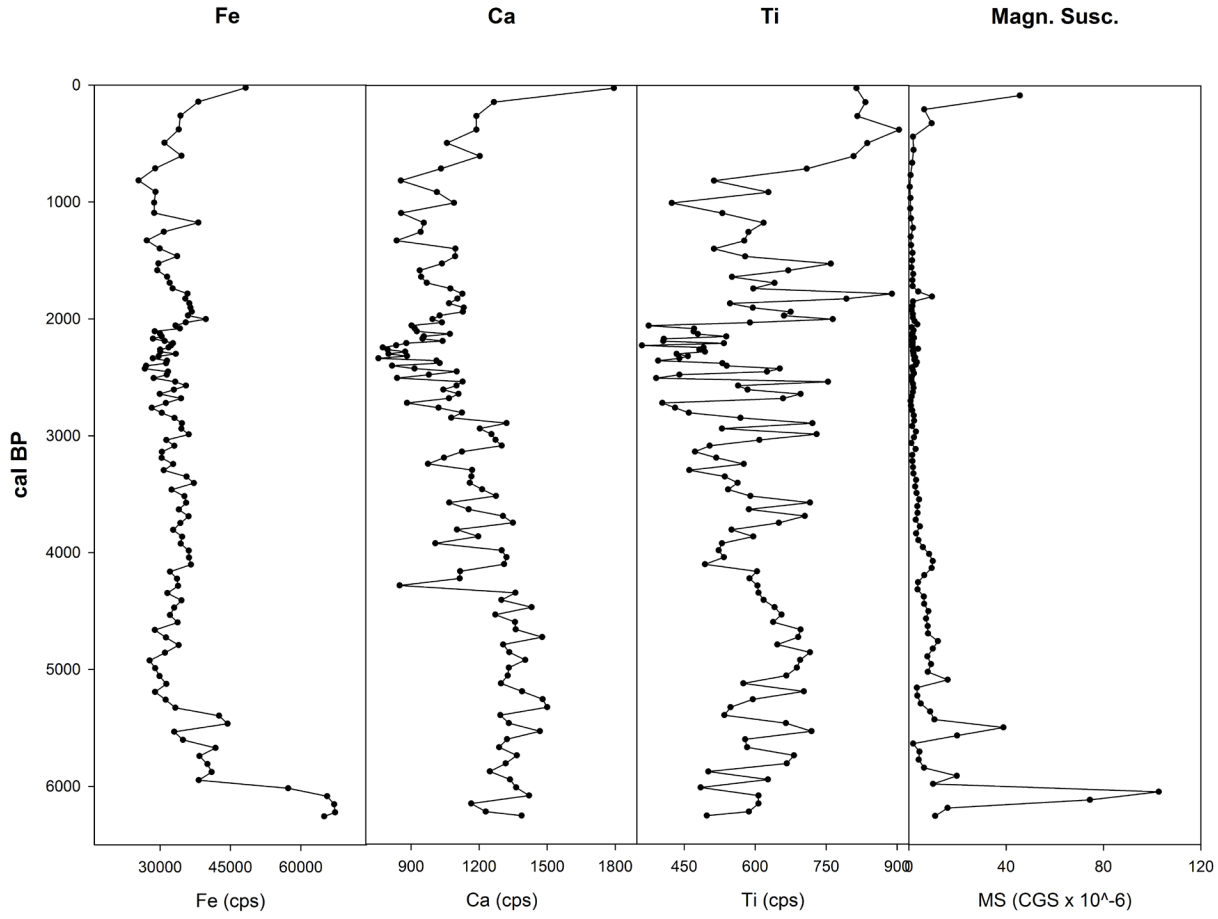

Figure 16. Down core profiles for Fe, Ca, Ti, and magnetic susceptibility for unit A (0 cm to 102.5 cm depth).

Elemental Correlation Matrices

Correlation matrices were constructed using the Itrax produced cps values in order to quantify the degree of association between pairs of elements present (Table 2). A single matric that compared elemental associations through the entire core was generated in addition to separate matrices for each lithostratigraphic unit, since considerable variation in composition and physical properties are observed between each unit. Strong ($r2 \geq 0.7$), positive correlations were observed between all 7 element over the entire record. Correlations that displayed $r2 \geq 0.9$ are highlighted with an asterisk. Through unit A, element were predominately weakly correlated. Only K:Ca, Ca:Sr. Ti:Sr, and Mn:Fe yielded correlations $r2 \geq 0.5$. Correlations were stronger in unit B (17 of 28 pairs displayed $r2 \geq 0.65$) and in unit C (16 of 28 pairs displayed $r2 \geq 0.65$). The only pairs of elements that correlated strongly in all three units were K:Ca, K:Sr, and Ca:Sr.

Variations in Elemental Composition: Unit A

In order to evaluate changes in elemental deposition over time, profiles were constructed to reflect elemental abundances as function of time using the smooth spline based age model (Figure 16). Iron ranged from 24364 to 165868 Fe/cps with a mean of 46904 Fe/cps. The Fe profile displayed high values at the bottom and top of unit A, which represented by the periods from 0-1,000 cal yr BP and from 5,000-6,200 cal yr B with the highest values observed in the latter. Prior to 1,000 cal yr BP, Fe values were higher from 1000-2100 cal yr BP. Calcium ranged from 726 to 13136 Ca/cps. Ca values were consistently higher from approximately 4500-6200 cal yr BP, before dropping significantly at approximately 4200 cal yr BP. Values stabilized afterwards, but continued to decrease through 2000 cal yr BP expect for a short period around 3000 cal yr BP that exhibited higher values. Since 1000 cal yr BP, values have been sharply increasing. The Titanium profile was much more variable than the other two profiles. Starting at the base of unit A, Ti values increased from 6000 cal yr BP through 4800 cal yr BP, after which values declined until around 3800 cal yr BP. From 3800 cal yr BP onward, values which much more variable. Notable high were observed at 3500 and 1500 cal yr BP, while lows are observed from 2000-2600 cal yr BP and at 1200 cal yr BP.From 1200 cal yr BP to the present, an increase in Ti is observed.

Organic Matter Analyses

Percent organic content, carbon, and nitrogen values throughout core ML-14-2 are shown in Figure 17 and 18. Percent organic content was determined based on %loss on ignition analysis that was performed at 1 cm intervals. The average LOI value for the entire core was 19.204 ± 9.26%, with a minimum of 0.342% at 138.5 cm and a maximum of 29.974% at 6.5 cm. In the basal clay (unit C), the organic matter content was 3.292 ± 1.93%. An increase in organic matter content is observed between unit C and the overlying transition layer (unit B) where it was 10.461 ± 4.67%. In unit B, the organic matter content was variable and oscillated between 2.295 and 15.798%. A sharp increase took place between the bottom two lithostratigraphic units and the top. Overall, organic content was much higher in unit A, which is described as an organic-rich gyttja. Organic content increased from 6200 to 4800 cal yr BP, but had low points at 4900 cal yr BP and 5400 cal yr BP. From %C and %N strongly correlated with percent organic content. %C and %N was lowest during the oldest part of the record (6250-4400 cal yr BP).

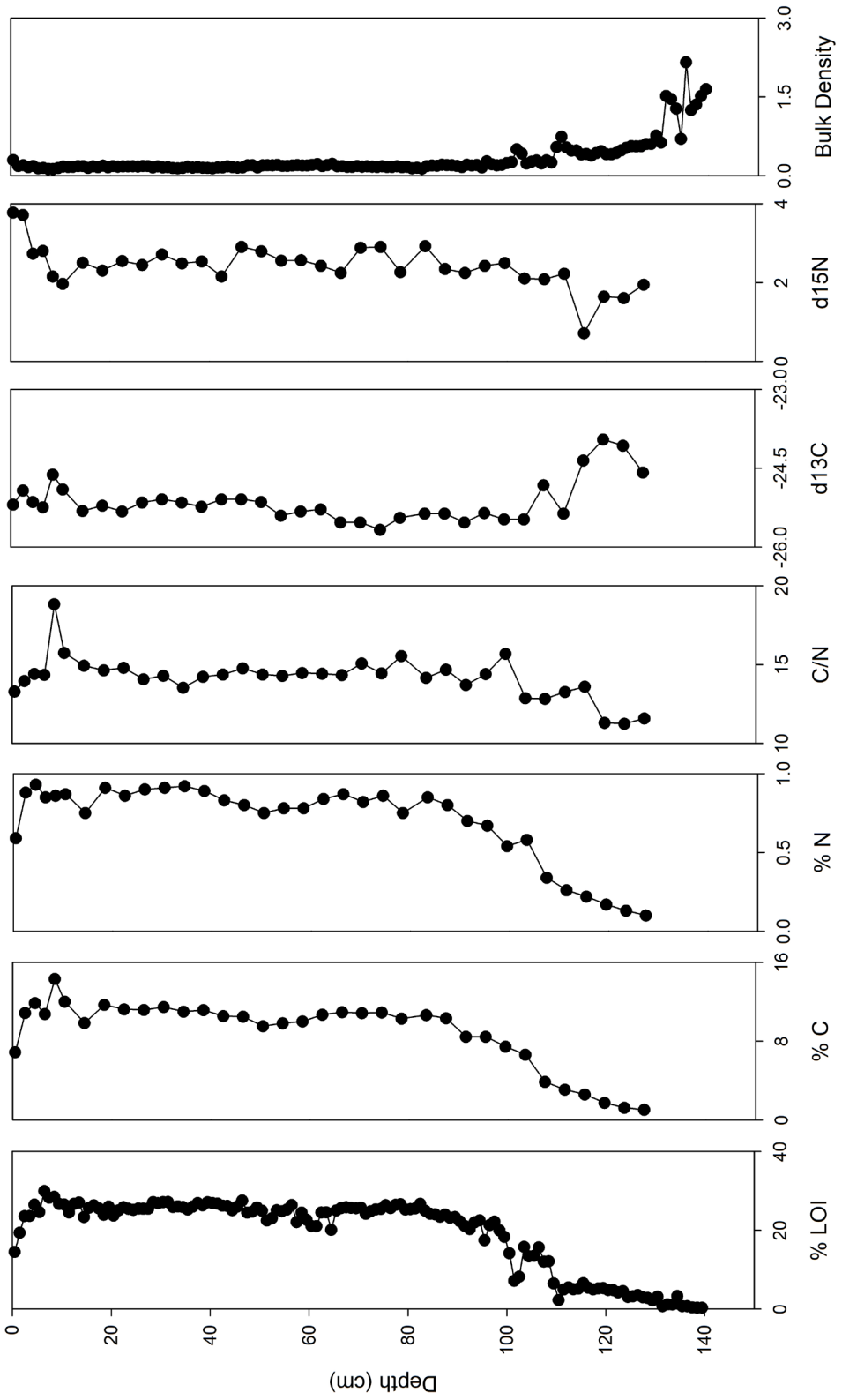

Figure 17. Down core profiles of the carbon analyes parameters plotted against depth (cm). Notice positive correlation between all paraments except for Bulk Density, which displays a negative correlation.

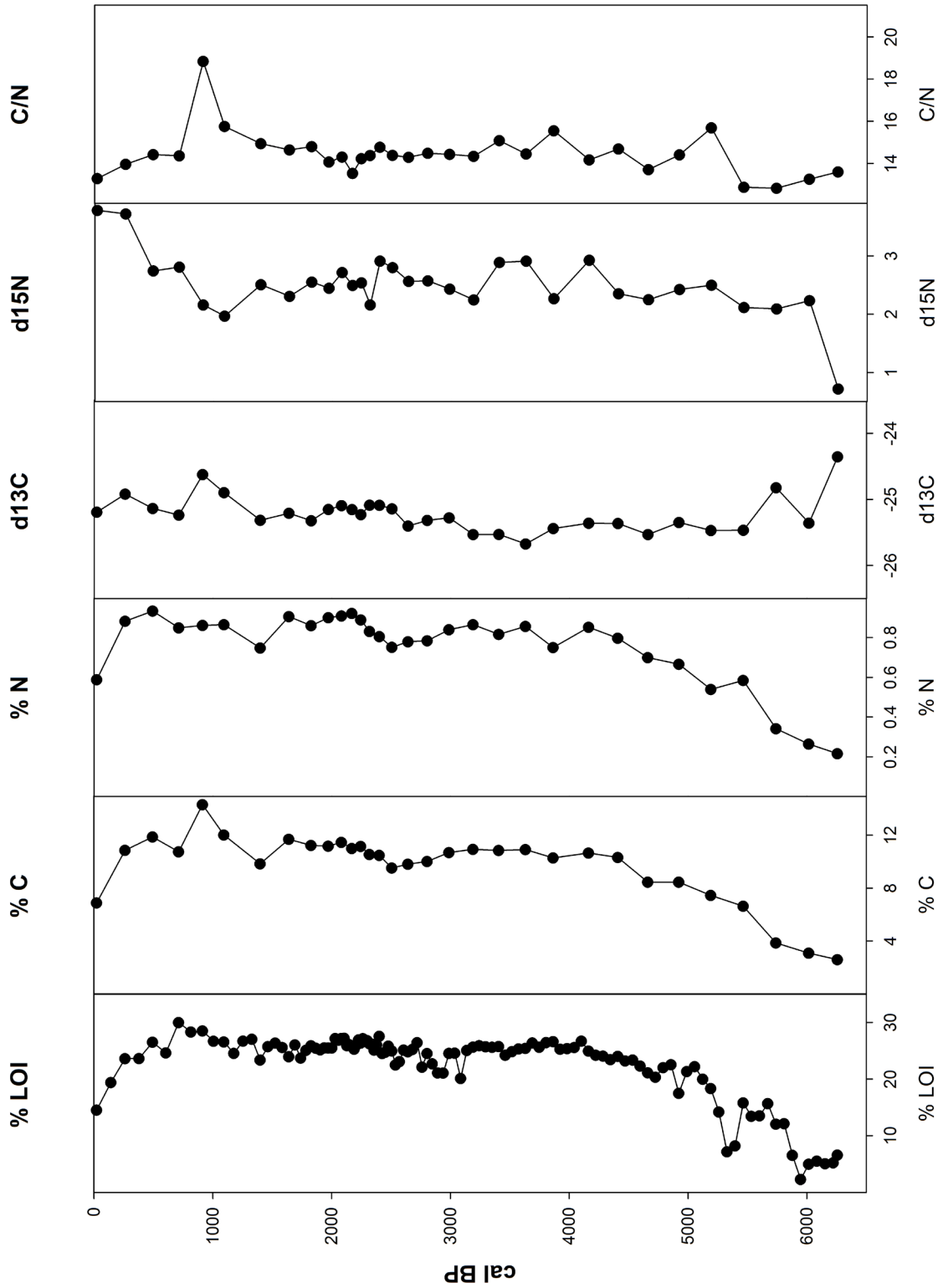

Figure 18. Down core profiles of the carbon analyes parameters plotted against age (cal yr BP). Notice positive correlation between all paraments except for Bulk Density, which displays a negative correlation.

relatively consistent with overall increasing trend. A small drop in values is observed at around 2500 cal yr BP followed by a notable drop at 1500 cal yr BP. A significant increase was observed at 800 cal yr BP only in the %C profile. Both %C and %N have decreased since 500 cal yr BP. The C/N values ranged from 11.24 to 18.84 and displayed an average of 14.19 ± 1.34. Notable peaks in the C/N are observed at 5190 and 900 cal yr BP. C/N values have gradually declined since this peak at 900 cal yr BP.

Chlorophyll Pigments

Total chlorophyll-a and phaeopigments abundances were measured at 2.0 cm resolution for core ML-14-2 (Figure 19). Chlorophyll-a values ranged from 382.82 to 46438.51 ug/g and averaged 11559.22 ug/g, while phaeopigments ranged from 1952.19 to 34766.93 ug/g. Total pigments (chlorophyll-a + phaeopigments) ranged from 408618 to 78531.28 ug/g. The chlorophyll-a contains three phases of productivity. From 139.5 cm to 103.5 cm, values were significantly higher and displayed large variation. A peak is noted at 109.5 cm. This trend is terminated by a drop in chlorophyll-a at 101.5 cm, after which values remained higher from 99.5 cm to 33.5 cm. During this period, values gradually declined from 91.5 cm. A period of lower values is observed from 31.5 cm to 17.5 cm depth, until values rose at 15.5 cm depth. Unlike the chlorophyll-a profile, the phaeopigments record exhibits only two different productivity signals, one from 139.5 cm to 102.5 cm and then another from 102.5 cm to the top of the core. Since chlorophyll-a pigment concentrations were higher, the total pigment profile more closely reflects changes in chlorophyll-a concentrations.

Sedimentation Rates

Mass accumulation rates (MAR) were calculated using the two age models and dry bulk density values presented previously. MARs were calculated by multiplying the linear accumulate rate (cm/yr, calculated by taking the age difference for each cm increase in depth) by the dry bulk density (g/cc), thereby generating a record for the mass of sediment that accumulates on 1 sq. cm of the lake bottom per year.

Summary of Results:

Abrupt transitions are observed between three different lithostratigraphic units are occur across the visual stratigraphy, physical properties, geochemical and paleo productivity proxies. These transitions are observed at depths of 102.5 cm and 111.5, which coincide with the 3 distinct units presented here. Considerable variability exists between each of the units. Unit A is characterized as a homogenous dark brown/black organic rich gyttja that displayed the highest compositions of organic content and relatively low elemental abundances. Unit B is observed a transition layer and contains a combination of properties the properties observed in unit A and C. In contrast to the top unit, unit C is predominately inorganic in compositions which is reflected in the organic matter profiles, magnetic susceptibility profiles, and XRF-elemental profiles. Higher concentrations of fossil pigemnts (chlorophyll-a + degradation products) were found in the inorganic unit than in the organic material.

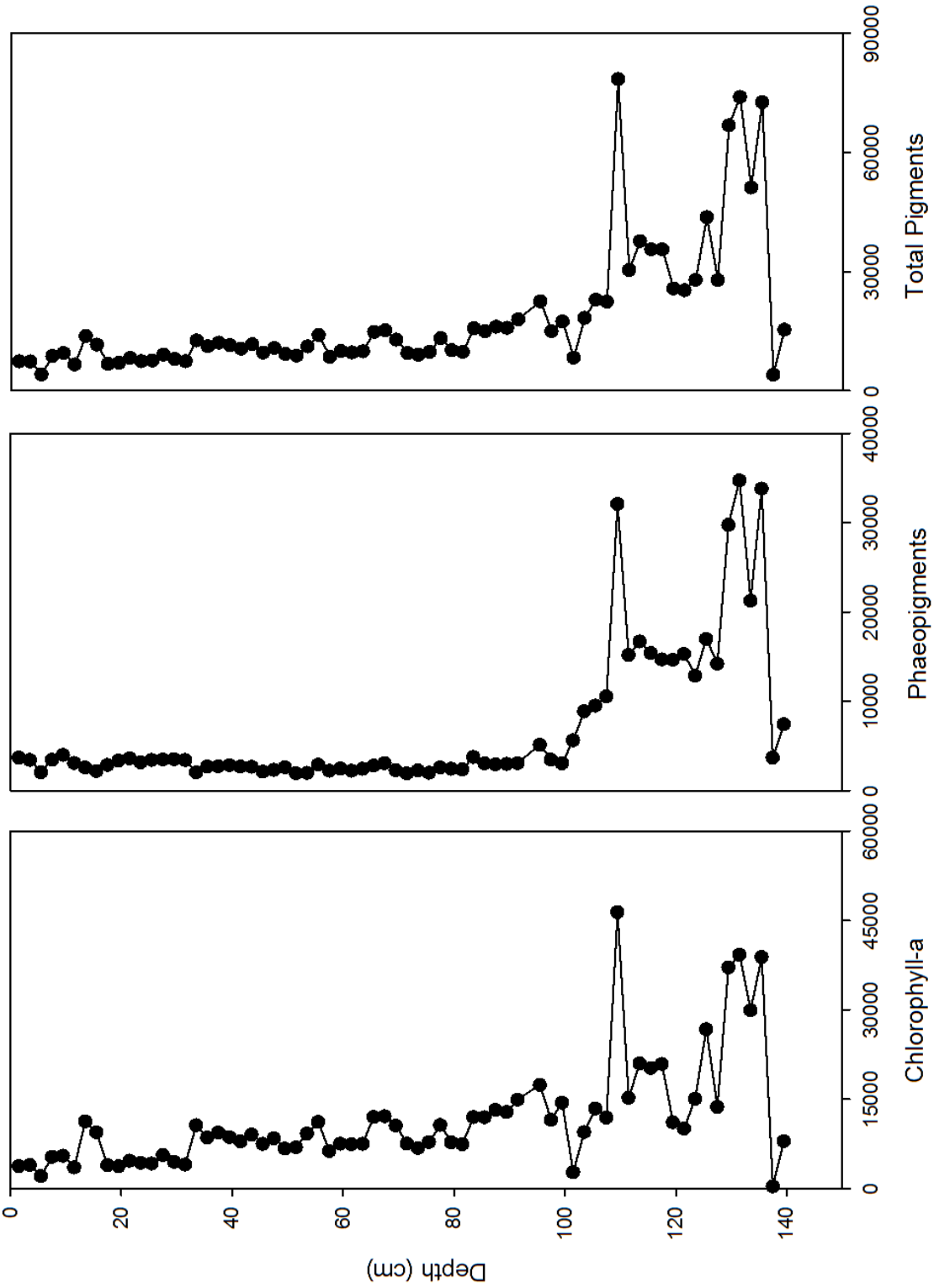

Figure 19. Down core profiles of fossil pigment concentrations (chlorophyll-a and its common degradation products. Two distinct units are observed as well as a decreasing trend up core starting at 100.5 cm depth.

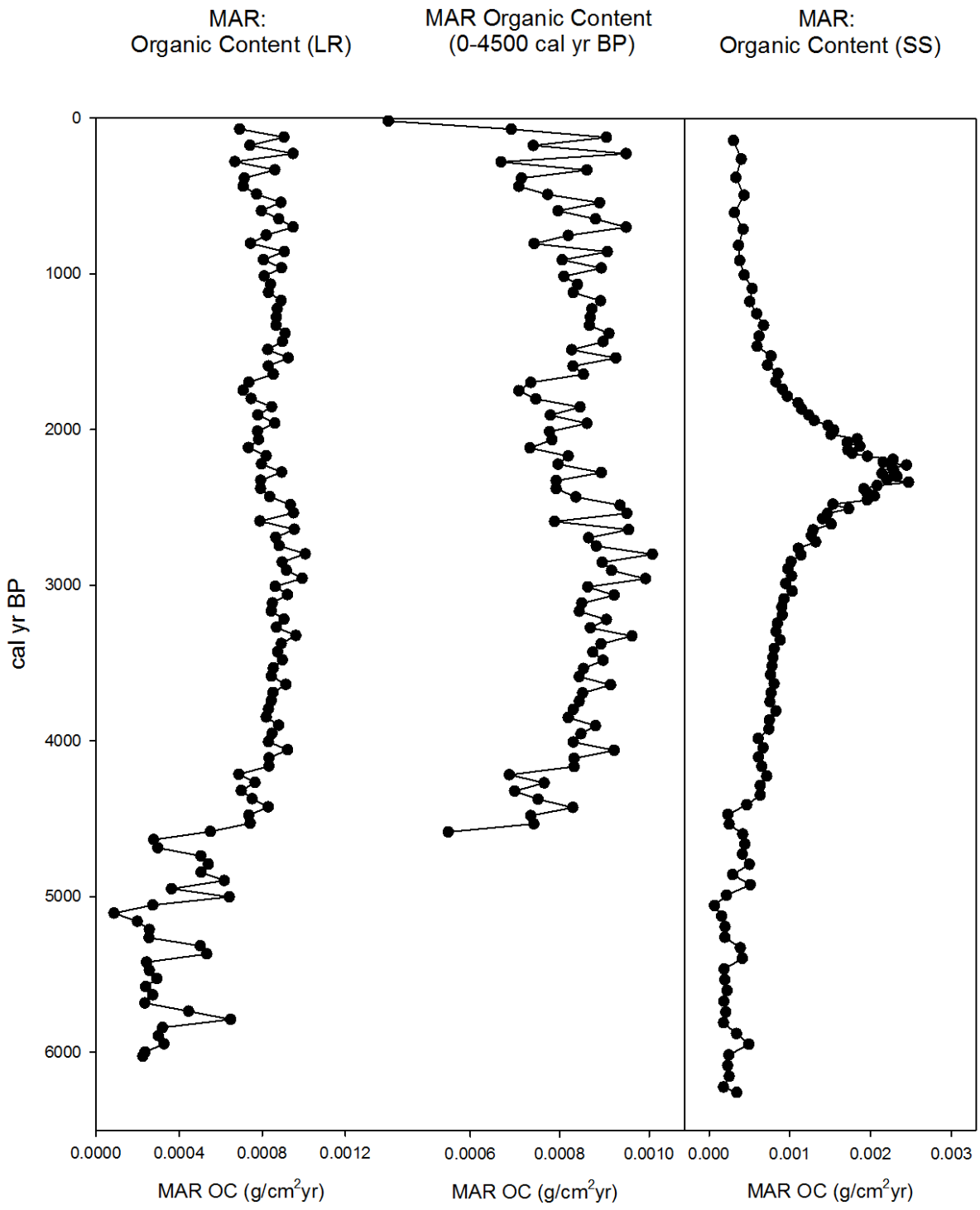

Figure 20. Profiles of mass accumulation rates of organic material using the two different age-depth models.

Discussion

Core Stratigraphy

Lakes act as natural traps for sediment and are thus able to integrate environmental and climatic forcings into a continuous, high-resolution archive of environmental change (Schnurrenberger et al., 2003). Lakes display significant variation based on origin, size, morphology, water chemistry, catchment size, and regional climate, which influence the nature and rate of sediment accumulation within the lacustrine basin. Since sediments accumulate at the bottom of lake basins, examining the composition of organic material may indicate changes in productivity and preservation conditions at the time of deposition, while inorganic sediments are primarily controlled by watershed erosion rates, storm events, and lake level.

Contained within the sediment core collected from Moose Lake (ML-14-2) are three distinct lithostratigraphic units: unit A, B, and C. The top unit (unit A) is described as a homogenous, organic rich gyttja that transitions into an inorganic, clastic unit containing both silt and clay (C). The transition layer, unit B, is a mosaic of units A and C. This visual classification based on visible interpretations of the core stratigraphy is further reflected by several geochemical analyses and productivity reconstructions used in this study, thus indicating a distinct environmental change occurred during this transition.

Organic Matter Provenance

Although organic matter only makes up a fraction of total lake sediments, the accumulation of organic material constitutes an important portion of overall sedimentation and contributes important information concerning the paleolimnologic record. The accumulation of organic matter within lacustrine environments is dependent on the types and amounts of material from primary sources as well as the extent of alteration and degradation of the original material (Meyers and Lallier-Verges, 1999). Organic material originates from either internal primary production (autochthonous) or imported from the catchment (allochthonous).

The organic matter analyses are shown in Figures 17 and 18, demonstrate that the concentrations of organic sediment (% LOI, % C, and % N) were significantly higher from the top of the core down to 102.5 cm (unit A) and were significantly lower in the bottom portion of the record (units B and C). Since % loss on ignition reflects the amount of organic matter in a sample, theoretically it is a good indicator of organic carbon content as well and is likely to change over time due to fluctuations in inorganic sediment input, productivity, and preservation conditions. Since the % C and % N profiles strongly correlated ($r2 \geq 0.93$) with the % LOI profile (showed higher values in unit A and decreased down core), it is assured that % LOI is a good indicator of organic carbon content and accumulation in lake sediments. % LOI was found to be approximately 41.9% C and 3.3% N. These initial observations find support in previous literature, which suggest that organic carbon is directly proportional to the abundance of total organic material and that organic carbon content in lake sediments can range from <1% upwards to 40% (Meyers and Teranes, 2001)

In order to understand the history of organic material accumulation within lakes, it is possible to distinguish the source of the organic material observed in the sediment as algal-produced (autochthonous) or vascular plants (allochthonous) and can be accomplished by interpreting the ratios of C/N and d13C values. Typically, lacustrine algae have low C/N ratios between 4 and 10, while terrestrial organic material from vascular plants have C/N ratios of 20 and greater (Meyers and Lallier-Verges, 1999). Additionally, d13C values for organic material produced from atmospheric CO2 by land plants using the C3 pathway has an average d13C of ca. -28%, whereas those utilizing the C4 pathway ca. -14% (O'Leary, 1988 from Meyers and Lallier-Verges, 1999). By plotting d13C values against C/N ratios, it may be possible to distinguish the source of organic material. Figure X indicates that Moose Lake accumulates organic material from a mixture of terrestrial C3 plants and lacustrine algae. The tight cluster of C/N ratios versus d13C values suggests that all of the organic material deposited during the period covered in this record (at least 6000 cal yr BP) is of the same origin. The few points that stray away from this cluster may indicate small shifts in the dominant material source. Such points are found along the bottom on the core, where the lowest C/N ratios are observed and may reflect a period where accumulation of algal-produced organic material was higher than the accumulation of material that was terrestrial in origin. Since this period is below the transition from unit B to C, no age estimates are available on these points. In contrast a notable peak in C/N ratio is observed at 10 cm (ca. 1000 cal yr BP) and may be a reflection of a period when the deposition of terrestrial organic material was the more dominant mechanism for organic matter accumulation.

Thus, a major shift in organic composition is seen, with higher concentrations of organic material found above 102.5 cm. Two theories can explain this abrupt transition. First, it is possible that there was a significant increase in productivity within the watershed. Increasing algal productivity within lakes occurs during times of wetter climates that transport a greater abundance of nutrients. It is also possible that there was a greater input of organic material from the terrestrial landscape. The second, theory that periods of lower organic material accumulation can be attributed to an increase in the flux of inorganic matter being deposited in the lake system.

Inorganic Sedimentary Sequence

Similarly to organic sediment, the properties of inorganic or clastic sediments archive important information concerning paleoenvironments and thus can be used to evaluate probable sources of accumulated sediment. For example records displaying low magnetic susceptibility values may indicate that less allochthonous inorganic material may have been transported and subsequently washed into the lake from the catchment these periods (Wetzel, 2001). Additionally, XRF elemental profiles provide semi-quantitative assessments of the concentrations of common rock forming elements, which provide valuable information concerning the geochemical properties of the sediment, the geology of the catchment, and the evolution of the lake system (Engstrom and Wright, 1984).

The magnetic susceptibility and XRF elemental profiles shown in Figures 15 and 16. Unlike the parameters examined in the organic analyses, bulk density, magnetic susceptibility, and XRF elemental profiles displayed higher values at the base of the core than at the top and were negatively correlated with the organic material parameters (% LOI, % C, and % N). Higher amounts of inorganic terrestrial sediment are observed in unit C, indicated by higher elemental peaks. This explains the increase in magnetic susceptibility since the most magnetically susceptible sediments

typically contain the highest amount of allochthonous inorganic material that has been washed into the lake basin. In unit A, however, both magnetic susceptibility and elemental peaks were significantly lower. The XRF elemental data displayed two distinct sequences as well and the strength of associations between the studies elements varied between the two sequences. From 102.5 to the bottom of the core, elemental associations were strongly correlated. Above 102.5 cm, however, associations were much weaker overall and none of the pairs indicated strong correlations. The coupling and decoupling of associated elemental pairs during these two sequences indicates a change in the depositional environment. Based on these profiles it seem that there was a change in the environmental conditions the caused a decrease in inorganic sedimentation after ca. 6000 cal yr BP that significantly reduced the amount of clastic sediment deposited into Moose Lake in the period that followed. The negative correlation between the XRF elemental profiles is not surprising since most of the elements measured by the XRF are going to be more abundant in clastic sediments since they are weathering products of either the local bedrock or soil erosion (Wetzel, 2001; Wilson, 2004; Anderson and Hawkes, 2003). In contrast, H, C, N, and Si elemental concentrations will be higher in the organic rich sediment. These elements associated with organic material is not measured by the XRF because they are too light and are below the detection limit for the instrument (Crodace et al., 2006) These observations suggest that from the base of the transition from inorganic, clastic sediment to organic rich gyttja at ca. 6000 cal yr BP (102.5 cm) to the present is a period of significantly higher biological productivity coupled with a greater deposition of organic material (Koff, 2012).

Based on the evidence suggested by these geochemical profiles, a major transition in the pattern of sedimentation is archived in this record. Sediment composition shifted from predominantly clastic sediment to organic rich gyttja up core. Two theories can help explain this transition. The first is that the increase in organic matter accumulation, due to increased productivity or more conducive preservation conditions, in unit A diluted the inorganic signal seen at the bottom of the core. Second, the rate or inorganic sediment accumulation significantly declined up core and permitted organic matter accumulation to be the dominant mechanism of sedimentation. Since C/N ratios indicate that the source of organic material consistently remained a mixture of aquatic algae and terrestrial plants, it is difficult to assume that an increase in aquatic productivity can account for the large increase in organic matter accumulation, exclusively. Since C/N ratios remain close, the deposition of organic matter of terrestrial origin must have increased as well to account for the increase in aquatic productivity. The more likely explanation is that the transition was caused by a reduction in the flux of inorganic sediment coupled with an increase of organic material input. Since sedimentation rates are extremely low, it is very unlikely that the organic signal was able to completely dilute the inorganic accumulation immediately after displaying % organic matter values of less than 5%.

Fossil Pigments and Paleoproductivity

As a proxy, fossil pigments are used to reconstruct changes in primary productivity within the lacustrine environments over time. Since almost all lakes along the tundra-boreal forest ecotone transition freeze over during the colder winter months, paleoproductivity reconstructions typically reflect changes in summertime productivity conditions, which can be used to make assumptions concerning temperature changes at a given time (Balter, 2014; D'Andrea et al., 2012). Fossil pigments, such as chlorophyll-a and its common degradation products, are often preserved in lake

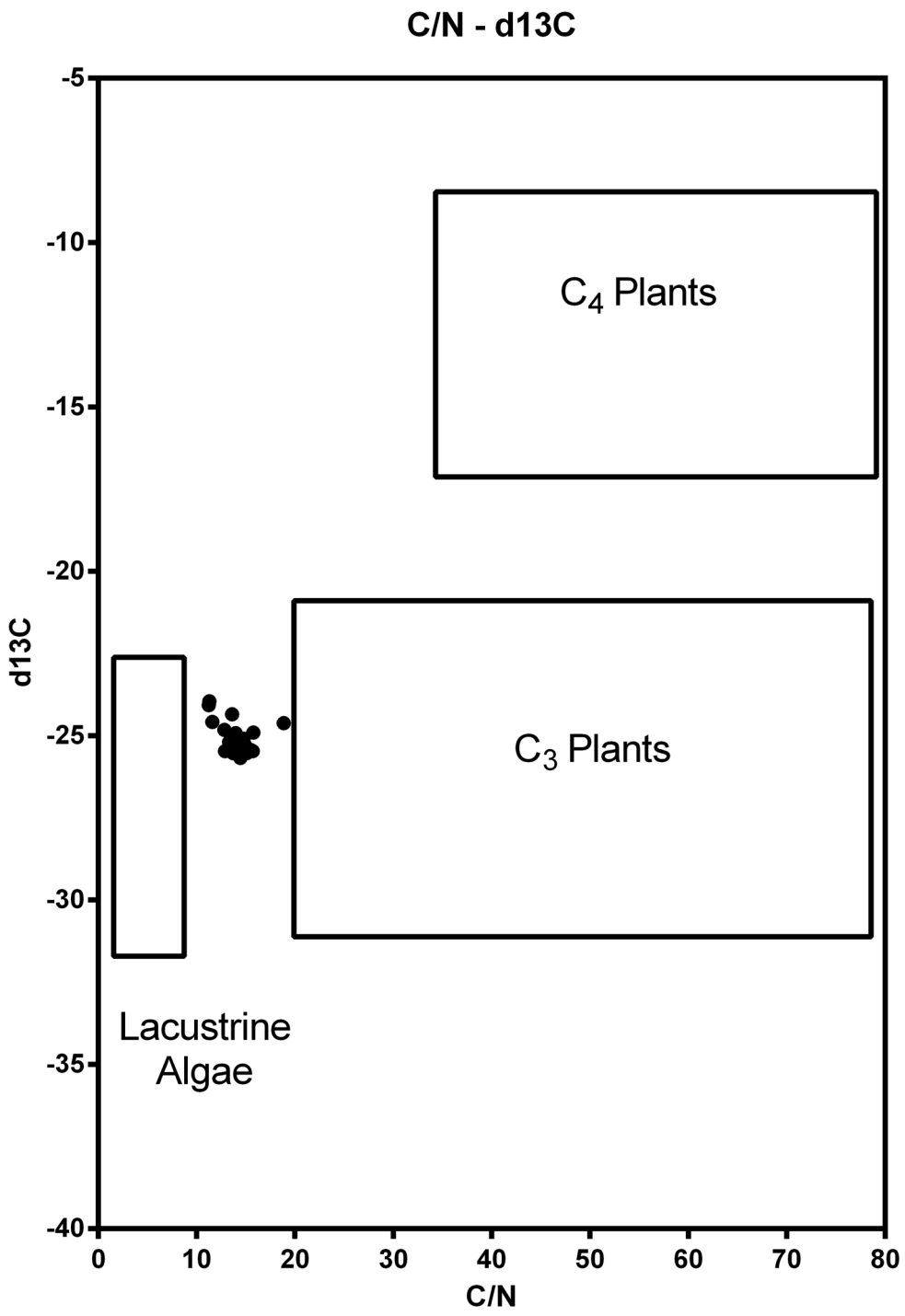

Figure 20: Plot showing the relationship between elemental and isotopic compositions of organic matter from lacustrine algae, C3 and C4 terrestrial plants. (from Meyers and Lallier-Vergès. 1999).

sediments, thus analyses of sedimentary chlorophylls and their derivatives can be used to reconstruct historical changes in primary production and be used to evaluate changes in temperature (Leavitt and Hodgson, 2001).

Landscape Evolution

The relative changes in total pigments are shown in Figure 17 and 18 and reflect changes in the observed lithostratigraphic units. Higher pigment concentrations are observed in unit C than in the top portion of the record. This contradicts an original assumption that lower rates of productivity would be observed in clastic dominant unit, while higher rates of productivity would be in the organic rich gyttja due to higher concentrations of organic matter. This assumption was based on a prevailing view that suggests lakes become more enriched with nutrients as they age, thus leading to increased biological production overtime (Michelutti et al., 2005). One explanation for the phenomenon displayed in this record, however, suggests that maximum pigment concentrations can be associated with early post-glacial periods as glaciers retreat following times dominated by tundra conditions (Wetzel, 2001; Engstrom et al., 2000; Milner et al., 2007). Based on the radiocarbon ages obtained from along the contact between gyttja and clastic sediment, it seems plausible that the record below 108.5 cm, reflects a post-glacial period following regional deglaciation of the Laurentide Ice sheet.

As stated above, a prevailing view holds that lakes become more enriched in nutrients as they age, leading to increased biological production, however, in a review of a series of lakes located in Glacier Bay, many lakes experienced an opposite evolution in which they grow more dilute and acidic with time, while accumulating dissolved organic carbon (Engstrom et al., 2000). This can be caused when a recently deglaciated terrain provides an initial surplus of nutrient loading due to soil development and woody biomass accumulation on land that is unmatched in streams or lakes (Milner et al., 2007). The early leaching of nutrients from the drainage basin increases phytoplankton productivity. Intermediate periods of relative stability or slowly declining rates of pigment deposition typically follow this initial surge and are controlled by variations in climate, rainfall, and nutrient conditions. As the forest and vegetation of the surrounding landscape reestablish, the high nutrient loading is reduced as does primary production. This trend is observed in the record. After displaying high overall concentrations of total pigments, pigment concentrations have been gradually declining since ca. 6000 cal yrs BP (102.5 cm). This indicates that during this portion of the record, productivity gradually declined and it is possible to infer that the reduced rates of productivity may be due to decreases in summertime temperature, since 59% of productivity change, which is reflected in pigments concentrations, can be attributed to changes in temperature (D'Andrea et al., 2012). It should be noted that when compared to down core organic content, total pigment concentrations a higher when organic content is low. This indicates that fossil pigments and aquatic productivity may not be a good predictor of organic content accumulation.

This hypothesis is further supported by the C/N ratio and d13C signal at the bottom of the record. In the final 6 cm of the core, C/N ratios declined and exhibited the lowest values observed throughout the core. d13C values increased and were less negative during this same period. This suggests a period when lacustrine algae were slightly more productive and a larger component of sediment organic matter during this period (Meyers and Lallier-Verges, 1999). Due to the high rate of inorganic sediment deposition, the signal of organic material produced by aquatic productivity was significantly diluted.

Temperature Interpretation

Since fossil pigments concentrations reflect rates of primary productivity, they are often used as a proxy to reconstruct temperature records. Two limitations restricted this from being accomplished in this study. First, since the modern instrumental record of climate for central Labrador begin in 1940, there is a lack of a high resolution temperature record available to correlate fossil pigment concentrations to. Second, due to low rates of sediment accumulation, the 2 cm sampling interval used in this analysis does not provide a high enough resolution record of paleoproductivity, thus these records only provide a general interpretation of productivity and therefore temperatures.

After displaying significantly high pigment concentrations in unit C, total pigment concentrations decreased significantly. However, after this initial drop, concentrations stabilized and gradually decreased up core. This trend is important to note, because it generally agrees with global temperature reconstruction for the past ca. 6000 cal BP. It has been suggested that following the warming associated with the Holocene thermal maximum (10,000 to 5,000 cal yr BP), global temperatures continued to decrease through the middle to late Holocene (Marcott et a., 2013). Although the physically stratigraphy does not seem support this trend, this paleoproductivity seems to agree that warmer temperatures were experienced in the earliest part of the record and temperatures have continued to cool since. No recent warming trend, associated with anthropogenic activity is observed, because of the sedimentation rates and subsequent low resolution record.

Considerations and Age Model Evaluation

In studies concerning paleoclimate reconstructions, the accurate dating of past events is of upmost importance since without the establishment of a reliable chronology it is impossible to determine whether events occurred synchronously as well as the rates at which environmental changes occurred (Bradley, 1999). Each of the two models developed in this study were constructed based on the seven ages obtained from AMS 14C radiocarbon dating.

Before discussing the results of the two age models that were constructed, a review of the assumptions incorporated and potential sources of errors must be presented. First, there is an apparent age reversal at the top of the core (7.5 and 15.5 cm depths). This suggests that either one or both of these ages is/are not valid. A potential explanation for this age reversal could be that the organic macrofossil (plant fragment) at 7.5 cm was an older fragment of organic matter that washed into the lake from the terrestrial landscape. This is important to note, since the radioactive "clock" begins as soon as the exchange of ^{14}C between the atmosphere and the organism terminates, which occurs when the terrestrial organism dies (Bradley, 1999). This means that the age reversal can be explained if the sample collected at 7.5 cm died at an older date, but took longer to be deposited into the lake basin. This could be due to its position in the watershed and greater distance to traverse. This same theory can be applied to the sample collected at 49.5 cm, which does not fit along the linear trend that can be made between the samples obtained from 15.5 cm, 35.5 cm, 76.0 cm, and 93.0 cm. The almost linear line suggests that the chronology in the early part of the record is accurate, but confidence declines through the upper part of the core.

The first attempt at developing an age model for this core was generated by linear interpolation. Despite the age reversal near the top of the sediment record, the fairly linear trend from the early through middle portions of the record suggests higher certainty in the accuracy of the age estimate

from the basal portion of the core (Figure X). The presence of the age reversal at the top suggests that one or both of the top two age estimates are incorrect. Another source of concern within this model is the steepness of the curve from approximately 35 cm – 50 cm, which indicates a significant increase in accumulation rates during this period. It is also plausible that this age model puts too much weight on the individual dates.

In order to address these uncertainties, two age models were developed for core ML-14-2 using two different modeling approaches: 1) a linear regression and 2) smooth spline curve. It is unlikely that a linear regression completely reflects sedimentation history since it suggests that accumulations rates have remained constant over the past 6000 years, which is most likely an inaccurate assumption. In contrast to going through all of the points, the smooth spline curve based age model avoids the upper most radiocarbon sample in order to account for the age reversal at the top of the core. This core has potential for being accurate, however, like the linear interpolation model, it requires that there be a significant increase in accumulation rate at ~2500 cal yrs BP followed by decrease in accumulation rate at ~2000 cal yrs BP.

Late-Holocene Sediment and Environmental History

As discussed previously, the sediment record from Moose Lake is composed of three contrasting stratigraphic units. Unit A is composed of an organic rich gyttja that exhibits low elemental cps values and magnetic susceptibility, while indicating a gradual decrease in phytoplankton productivity up core. Unit B and C displayed similar results that consisted of high magnetic susceptibility and high elemental peaks. Organic content was low (less than 1% towards at the bottom of the core). Contrary to prevailing view, chlorophyll-based phytoplankton productivity was significantly higher in this unit, despite it being predominantly inorganic. Based on the conditions, it is clear that the remote subarctic Moose Lake has experienced marked environmental change throughout the record. Here it is proposed that Moose Lake and its associated watershed experienced a landscape evolution similar to the one described by Milner et al. (2007), in which the environment developed from physical controlled to biotic controlled following deglaciation. Following ice recession, soil development and biomass accumulation on land provided an inertia that

This transition from organic-rich sediment to basal clay shows characteristics of activity associated with deglaciation or a post-glacial system. The basal calibrated radiocarbon age obtained from an organic macrofossil found along this transition zone (107.5 cm) organic matter directly overlying the transition from inorganic sediments place this transition at 5848.5 cal yrs BP, thus suggesting that the record presented in core ML-14-2 history covering the periods of post-glacial and into the late Holocene.

The date on this transition, however, raises some doubts since it has been suggested that southeastern Labrador experienced deglaciation of the Laurentide Ice Sheet between 8 and 9 kyr BP and only northern Quebec and Labrador was able to retain ice 6 kyr BP and into the Holocene Thermal Maximum (Kaufman et al., 2004). Results proposed by Occhietti et al. (2004 & 2011) and King (1985) suggest that the lowlands located to the south of the Mealy Mountains would have been deglaciated by 9-10 kyr BP, however, the west end of Lake Melville was not ice free until 7.5 kyr BP. In a pollen-based paleoclimate reconstruction study, Kerwin et al. (2004) found that summertime temperatures were 1-2°C cooler than present in Quebec and Labrador prior to 6 ka and it was only

after the residual Laurentide Ice Sheet had melted that modern temperature values were reached. During this same period, the retreat of the Laurentide Ice Sheet accounted for a significant rise in sea level. As the ice sheet retreated, the ocean flooded the glacio-isostatically depressed Labrador coast, causing marine limits to reach elevations of 152 m asl in southern Labrador (Smith et al., 2003). This indicates that during this period, summertime temperatures would have been cooler through the early Holocene and that winters could have been wetter since the coast was closer. It is also possible that the pieces of the residual ice sheet could have influenced local atmospheric circulation patterns and produced cooler temperatures for the region.

Based on this evidence, it seems plausible that the higher elevations of the Mealy Mountains could have retained ice into the mid-Holocene during the thermal maximum. The timing of this transition from inorganic-rich clastic sediment to organic gyttja is supported by based on pollen records collected elsewhere in Labrador (Fallu et al., 2004; Lamb, 1980; Kerwin et al., 2004). Additional support is found in the presence of many end moraines located at the base of some of cirques located in the study area, which suggests that is possible that local ice could have persisted within the area after regional deglaciation had occurred (Gray, 1969).

The lack of an anthropogenic induced productivity signal and increased accumulation of organic material is most likely due to reasons. First, the low annual resolution prevents it from being visible. Second, the lakes of the Mealy Mountains have remained pristine and do not host standing populations or many visitors annually. Although the Mealy Mountains have a long standing tradition of seasonal land use by the Labrador Innu, the majority of substance resource extraction is restricted to areas of lower elevation than this study site (Trant and Hermanutz, 2014).

Organic Matter Mass Accumulation Rate

It has been suggested that lake sediments serve as important reservoirs for the accumulation of organic carbon by accumulating 50% of the annual accumulation in marine sediments, despite covering less than 2% of the Earth's surface (Dean and Gorham, 1998). Despite high overall rates of accumulation, significant variation in accumulation rates between different lakes has been observed on several of magnitude (Kortelainen et al., 2004). In summary, it seems that the burial efficiency of organic carbon in lakes is dependent on oxygen availability, since anoxic conditions favor organic carbon preservation (Alin and Johnson, 2007; Maerki et al., 2009; Sobek et al., 2009). To date, however, the factors controlling burial efficiency and accumulation of organic carbon continue to be poorly understood, while questions remain concerning the sensitivity of these rates to change over time.

In the previous sections, the differences between the different lithostratigraphic units were evaluated and possible explanations for their appearance in the record were presented, however, these explanation do not address two of the essential questions driving this investigation: 1) how do mass accumulation rates of organic carbon change over time and 2) how sensitive are these rates to changing climate conditions.

The mass accumulation rates of organic material (MAR) for Moose Lake were reconstructed using the sedimentation rates that are based on the two age models and bulk densities presented earlier. Using the sediment accumulation rates and % LOI, it was possible to determine the mass accumulation rate of organic matter. % LOI was used as a proxy for organic carbon, since a higher resolution profile was constructed and the strong correlation was observed between % LOI and % C

indicates that % LOI is a good proxy for organic carbon content.

The mass accumulation rates of organic matter profiles are shown in Figure 20. This suggests that a peak in mass organic carbon accumulation occurred between 3000 and 2000 cal yr BP (Figure X). However, the overall shape of the smooth spline constructed curve almost purely reflects the change in the shape of the original age-depth curve, while only slightly reflecting variations in % LOI. This occurs even though, there is no evidence indicating that a significant change in lithology occurs at that depth that could explain the substantial increase (2-3 times increase) in accumulation rates. Instead, profiles remain pretty consistent through that part of the record. It is possible that the overall shape of this curve relates back to the problems and uncertainties posed by the radiocarbon age estimates of the samples dated above 40 cm.

In contrast to the smooth spline MAR, the linear regression generated MAR profiles assumes that the sedimentation rates remained constant throughout the record (0.019 cm/yr and 0.00413 g/cm^{2}yr). Although there is no indication from past studies that sedimentation remains constant throughout history, the sedimentation rate of 0.19 cm/yr is quite similar to other sediment accumulation rates observed for other lakes located in subartic with tundra like conditions (Crann et al., 2014). Although these are relatively low rates of accumulation, they are not unreasonable since the watershed surrounding Moose Lake is small. Additionally Moose Lake is a very clear and clean lake, and relatively deep, which indicates that productivity within the lake is relatively low to begin with. Since the catchment is small and the surrounding vegetation is characteristic of an alpine tundra, the input of allochthonous material will be small as well. Thus, it seems that accumulation rates are low due to low rates of primary productivity in addition to low rates of deposition from organic material from terrestrial sources. Low accumulation rates due to low productivity and low rates of terrestrial transport. Although the mass bulk accumulation rate (g/cm^{2}yr) displayed higher rates towards the bottom of the record, due to an overall increase in sediment density, organic matter MAR exhibited increasing rates up core due to increasing organic content observed in the upper portion of the profile. This suggests that although it is unlikely that sediment accumulation rates were constant for the entire record, the linear regression model is more sensitive to changes in organic content in its associated MAR curve, unlike the smooth spline curve. This suggest that the linear regression curve might be a better alternative in evaluating changes in accumulation rates over time.

Conclusion

Contained within the sediment core collected from Moose Lake (ML-14-2) are three distinct lithostratigraphic units: unit A, B, and C. The top unit is described as a homogenous, organic rich gyttja that transitions into an inorganic, clastic unit containing both silt and clay. This visual classification of the core stratigraphy is further reflected by the several geochemical analysis used in this study. Common mineral forming elements displayed higher values along the bottom of the core than at the top, which most likely originated from unconsolidated glacial deposits (Milner et al., 2007). In contrast, % LOI, % C, and % N were higher at the top of the core. Fossil pigments were used to reconstruct paleoproductivity and show higher concentrations at the bottom of the core. It is believed that producitivity increased during this time in result of nutrient loading available following deglaciation. By the time the forest and vegetation had reestablished, nutrint loading had declined. Two age-depth models were used to reconstruct mass accumulation rates of organic material to simulate organic carbon. Of the two curves used, the linear regression curve seemed to reflect changes in organic content the best. Future work should be targeted at constructing a higher resolution record paired with a more accurate age-depth model in order to accurately evaluate changes in sediment accumulation.

Bibliography

Anderson, D.H., Hawkes, H.E., 2003. Relative mobility of the common elements in weathering of some schist and granite areas: Geochicmica et Cosmoschima Acta Vol. 14, No. 3, p. 204-210.

Croudace, I.W., Rindby, A., Rothwell, R.G., 2006, ITRAX: description and evaluation of a new multi-function X-ray core scanner: New Techniques in Sediment Core Analysis, Geological Society, London, Special Publications, Vol 267, p. 51-63.

Carcaillet, C., Richard, P.J.H., 2000. Holocene changes in seasonal precipitation highlighted by fire incidence in eastern Canada. Climate Dynamics, Vol. 16, p. 549-559.

Banfield, C.E., and Jacobs, J.D., 1998, Regional Patterns of Temperature and Precipitation for Newfoundland and Labrador during the past Century: The Canadian Geographer, Vol. 42, No. 4, p. 354-364.

Blaauw, M., 2010. Methods and code for 'classical' age-modeling of radiocarbon sequences: Quaternary Geochronology Vol. 5, p. 512-518.

Carlson, A.E., and Clark, P.U., 2007. Rapid Holocene Deglaciation of the Labrador Sector of the Laurentide Ice Sheet: Journal of Climate, Vol. 20, p. 5126-5133.

Clark, C.D., Knight, J.K., and Gray, J.T., 2000, Geomorphological reconstruction of the Labrador Sector of the Laurentide Ice Sheet: Quaternary Science Reviews, Vol. 19, p. 1343-1366.

Cole, J.J., Prairie, Y.T., Caraco, N.F., McDowell, W.H., Tranvik, L.J., Striegl, R.G., Duarte, C.M., Kortelainen, P., Downing, J.A., Middleburg, J.J., and Melack, J., 2007, Plumbing the Global Carbon Cycle: Integrating Inland Waters into the Terrestrial Carbon Budget: Ecosystems, Vol. 10, p. 171-184.

Crann, C.A., Patterson, R.T., Macumber, A.L., Galloway, J.M., Roe, H., Blaauw, M., Swindles, G.T., Falck, 2014. Sediment accumulation rates in subartic lakes: Insights into age-depth modeling from 22 dated lake records from the Northwest Territories, Canada.

Dean, W.E., 1999, The carbon cycle and biogeochemical dynamics in lake sediments: Journal of Paleolimnology, Vol. 21, p. 375-393.

D'Arrigo, R.D., Buckley, B., Kaplan, S., and Woollett, J., 2003, Interannual to multidecadal modes of Labrador climate variability inferred from tree rings: Climate Dynamics, Vol. 20, 219-228.

Engstrom, D.R., 1984, Lake Development in the Boreal Peatlands of Southeastern Labrador, Canada: Arctic and Alpine Research, Vol. 16, No. 4, p. 447-452.

Han, G., 2005, Wind-driven barotropic circulation off Newfoundland and Labrador: Continental Shelf Research, Vol. 25, p. 2084-2106.

Gower, C.F. and van Nostrand, T., 1996, Geology of the southeast Mealy Mountains region, Greenville Province, Southeast Labrador: Current Research, Report 96-1, p. 55-71.

Gray, J.T., 1969, Glacial History of the Eastern Mealy Mountains, Southern Labrador: Arctic, Vol. 22, No. 2, p. 106-111.

Gudasz, C., 2011. Boreal lake sediments as sources and sinks of carbon. Summaries of Uppsala

Dissertations from the Faculty of Science and Technology, Vol. 823, p. 39.

Fallu, M., Pienitz, R., Walker, I.R., Lavoie, M., 2005. Paleolimnology of a shrub-tundra lake and response of aquatic and terrestrial indicators to climate change in arctic Quebec, Canada: Paleoogeography, Palaeoclimatology, Palaeoecology, Vol. 215, 183-203.

Ferland, M.E., Prairie, Y.T., Teodoru, C., and del Giorgio, P.A., 2014, Linking organic carbon sedimentation, burial efficiency and long-term accumulation in boreal lakes: Journal of Geophysical Research Biogeosciences, Vol. 219, p. 836-847.

Jacobs, J.D., Chan, S., and Sutton, E., 2014, Climatology of the Forest-Tundra Ecotone at a Maritime Subarctic-Alpine Site, Mealy Mountains, Labrador: Arctic, Vol. 67, No. 1, p. 28-42.

James, D.T., and Nadeau, L., 2001: Geology of the little mecatina river (NTS map area 13D/NE) and LAC arvert (NTS map area 13C/SW) areas, Greenville Province, Southern Labrador: Newfoundland Department of Mines and Energy Geologic Survey, Report 2001, p. 55-73.

Kaufman, D.S., Schneider, D.P., McKay, N.P., Ammann, C.M., Bradley, R.S., Briffa, K.R., Miller, G.H., Otto-Bliesner, B.L., Overpeck, J.T., Vinther, B.M., and Arctic Lakes 2k Project Members, 2009, Recent warming reverses long-term arctic cooling: Science, Vol. 325, p. 1236-1239.

Kerwin, M.W., Overpeck, J.T., Webb, R.S., Anderson, K.H., 2004. Pollen-based summer temperature reconstructions for the eastern Canadian Boreal forest, subarctic, and Arctic: Quaternary Science Reviews, Vol. 23, p. 1901-1924.

Koff, A.T., (2012) A multi-proxy paleolimnological study of Holocene Sediments in Missisquoi Bay, USA-Canada. Masters Thesis University of Vermont, p. 1-144.

Kylander, M.E., Ampel, L., Wohlfarth, B., Veres, D., High-resolution X-ray fluorescence of Les Echets (France) sedimentary sequence: new insights from chemical proxies. Journal of Quaternary Science, Vol. 26, No. 1, p. 109-117.

Michelutti, N., Wolfe, A.P., Vinebrook, Rolf, D., Rivard, B. 2005. Recent primary production increases in arctic lakes. Geophysical Research Letters, Vol. 32, p. 1-4.

Marcott, S.A., Shakun, J.D., Clark, P.U., and Mix, A.C., 2013, A Reconstruction of Regional and Global Temperature for the Past 11,300 Years: Science, Vol. 339, p. 1198-1201.

Meyers, P.A., and Lallier-verges, E., 1999, Lacustrine Sedimentary Organic Matter Records of Lake Quaternary Paleoclimates: Journal of Paleolimnology, Vol. 21, No. 3, p. 345-372.

Mulholland, P.J. and Elwood, J.W., 1982, The role of lake and reservoir sediments as sinks in the perturbed global carbon cycle: Tellus, Vol. 34, p. 490-499.

Reimer, P.J., Bard, E., Bayliss, A., Beck, J.W., Blackwell, P.G., Bronk Ramsey, C., Buck, C.E., Edwards, R.L., Friedrich, M., Grootes, P.M., Guilderson, T.P., Haflidason, H., Hajdas, I., Hatte, C., Heaton, T.J., Hoffman, D.L., Hogg, A.G., Hughen, K.A., Kaiser, K.F., Kromer, B., Manning, S.W., Niu, M., Reimer, R.W., Richards, D.A., Scott, E.M., Southon, J.R., Turney, C.S.M., van der Plicht, J., 2013. IntCal13 and Marine13 radiocarbon age calibration curves, 0-50,000 years cal BP. Radiocarbon 55: 1869-1887.

Schindler, D.W., 2009, Lakes as sentinels and integrators for the effects of climate change on watersheds, airsheds, and landscapes: Limnology and Oceanography, Vol. 54, No. 6, p. 2349-2359.

Sobek, S., Durisch-Kaiser, E., Zurbrugg, R., Wongfun, N., Wessels, M., Pasche, N., and Wehrli, R., 2009,

Organic carbon burial efficiency in lake sediments controlled by oxygen exposure time and sediment source: Limnology Oceanography, Vol. 54, No. 6, p. 2243-2254.
Schnurrenberger, D., Russell, J., Kelts, K., 2003. Classification of lacustrine sediments based on sedimentary components. Journal of Paleolimnology, Vol. 29, p. 141-154.

Trant, A.J., Hermanutz, L, (2014) Advancing towards novel tree lines? A multispecies approach to recent tree line dynamics in subarctic alpine Labrador, northern Canada. Journal of Biogeography, 1-11.

Williamson, C.E., Saros, J.E., Vincent, W.F., and Smol, J.P., 2009, Lakes and reservoirs as sentinels, integrators, and regulators of climate change: Limnology and Oceanography, Vol. 54, No. 6, p. 2273-2282.

Williamson, C.E., Saros, J.E., and Schindler, D.W., 2009, Sentinels of Change: Science, Vol. 323, p. 887-888.

Wilson, M.J. (2004) Weathering of primary rock-forming minerals: processes, products, and rates. Clay Minerals, 39: 233-266.

.